





Heat-related changes in the velocity and kinetic energy of flowing blood influence the human heart's output during hyperthermia

Kazuhito Watanabe^{1,2} , Nuno Koch Esteves^{1,3} , Oliver R. Gibson^{1,4}, Koichi Akiyama⁵ , Sumie Watanabe^{1,2} and José González-Alonso¹ 

¹Division of Sport, Health and Exercise Sciences, Department of Life Sciences, Brunel University London, Uxbridge, UK

²Faculty of Education and Human Studies, Akita University, Akita, Japan

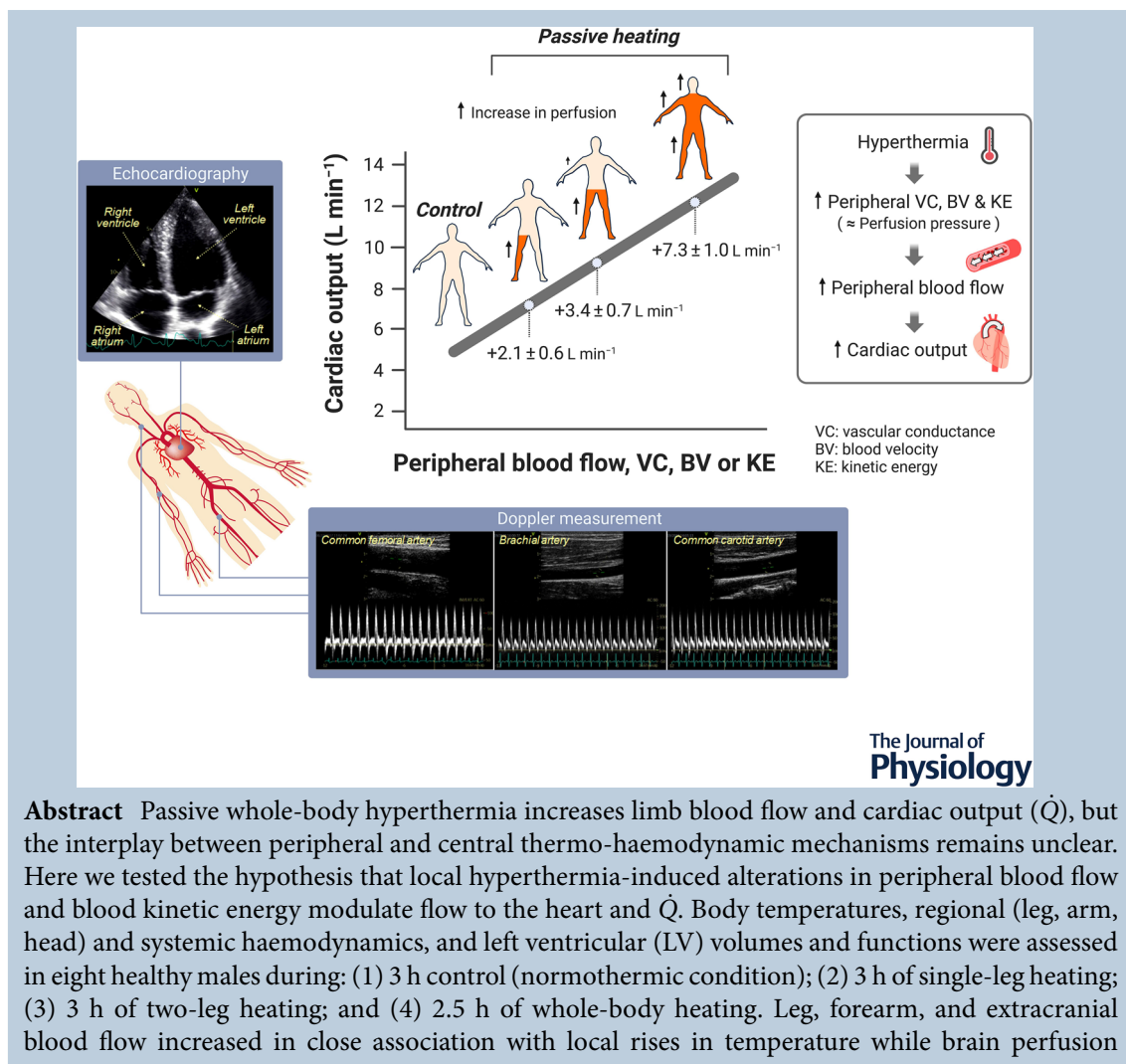
³Research Centre, University College of Osteopathy, London, UK

⁴Centre for Physical Activity in Health and Disease, Brunel University London, Uxbridge, UK

⁵Department of Anesthesiology, Kindai University Hospital, Osaka, Japan

Handling Editors: Bjorn Knollmann & Igor Fernandes

The peer review history is available in the Supporting information section of this article (<https://doi.org/10.1113/JP285760#support-information-section>).



remained unchanged. Increases in blood velocity with small to no changes in the conduit artery diameter underpinned the augmented limb and extracranial perfusion. In all heating conditions, \dot{Q} increased in association with proportional elevations in systemic vascular conductance, related to enhanced blood flow, blood velocity, vascular conductance and kinetic energy in the limbs and head (all $R^2 \geq 0.803$; $P < 0.001$), but not in the brain. LV systolic (end-systolic elastance and twist) and diastolic functional profiles (untwisting rate), pulmonary ventilation and systemic aerobic metabolism were only altered in whole-body heating. These findings substantiate the idea that local hyperthermia-induced selective alterations in peripheral blood flow modulate the magnitude of flow to the heart and \dot{Q} through changes in blood velocity and kinetic energy. Localised heat-activated events in the peripheral circulation therefore affect the human heart's output.

(Received 3 October 2023; accepted after revision 3 April 2024; first published online 1 May 2024)

Corresponding author K. Watanabe: Faculty of Education and Human Studies, Akita University, Akita City, Akita, 010-8502, Japan. Email: k.watanabe@ed.akita-u.ac.jp

Abstract figure legend We investigated the regional (leg, arm and head) and systemic haemodynamics during passive single-leg, two-leg and whole-body hyperthermia to test the hypothesis that the increase in cardiac output (\dot{Q}) with hyperthermia is closely related to elevations in peripheral haemodynamics rather than changes in central haemodynamic forces and factors. Single-leg, two-leg, and whole-body hyperthermia induced graded increases in \dot{Q} , tightly associated with increased peripheral (limbs and head) blood flow, vascular conductance (VC), blood velocity (BV) and kinetic energy (KE). Our findings suggest that central forces and factors related to cardiorespiratory and metabolic activities, such as alterations in pressure propulsion and left ventricular function, are not obligatory for increasing \dot{Q} during passive hyperthermia. This highlights the importance of heat-activated events in periphery in the control of blood circulation during hyperthermia.

Key points

- Local and whole-body hyperthermia increases limb and systemic perfusion, but the underlying peripheral and central heat-sensitive mechanisms are not fully established.
- Here we investigated the regional (leg, arm and head) and systemic haemodynamics (cardiac output: \dot{Q}) during passive single-leg, two-leg and whole-body hyperthermia to determine the contribution of peripheral and central thermosensitive factors in the control of human circulation.
- Single-leg, two-leg, and whole-body hyperthermia induced graded increases in leg blood flow and \dot{Q} . Brain blood flow, however, remained unchanged in all conditions. Ventilation, extracranial blood flow and cardiac systolic and diastolic functions only increased during whole-body hyperthermia.
- The augmented \dot{Q} with hyperthermia was tightly related to increased limb and head blood velocity, flow and kinetic energy.
- The findings indicate that local thermosensitive mechanisms modulate regional blood velocity, flow and kinetic energy, thereby controlling the magnitude of flow to the heart and thus the coupling of peripheral and central circulation during hyperthermia.

Kazuhito Watanabe is an associate professor in the Faculty of Education and Human Studies at Akita University. The study described in the present manuscript represents research conducted as part of his post-doctoral training at Brunel University London, under the guidance of Professor José González-Alonso. His research interests encompass integrative human cardiovascular control during exercise and environmental stress, with a particular focus on understanding the role of the heart and the periphery in the control of blood circulation.



Introduction

Increases in body temperature elicit profound alterations in peripheral and central haemodynamics. During thermal interventions evoking progressive hyperthermia at rest (i.e. passive hyperthermia), cardiac output (\dot{Q}) increases by $\sim 3 \text{ L min}^{-1}$ for every 1°C rise in core temperature, and the magnitude of the elevation can be $>5 \text{ L min}^{-1}$ during severe whole-body hyperthermia with arterial pressure remaining stable or declining slightly (Chiesa et al., 2016, 2019; Minson et al., 1998; Rowell et al., 1969; Stöhr, González-Alonso, Pearson et al., 2011). According to the conventional view of blood circulation, central haemodynamic forces evoked by the pressure-generating function of the heart are the principal determinants of blood flow distribution to the peripheral tissues and organs (Rowell, 1993; Secomb, 2016). In this cardiocentric construct, the elevated heart rate (HR) is the key factor increasing \dot{Q} and the heart is the primary organ generating the mechanical energy (pressure energy) to increase peripheral blood flow during hyperthermia. However, contention arises given that classic observations in the isolated mammalian heart demonstrate that the rise in blood temperature linearly increases HR, but does not alter \dot{Q} because of the proportional reduction in stroke volume (SV) (Knowlton & Starling, 1912). A similar phenomenon has been observed in human studies where HR was increased using cardiac pacing (Bada et al., 2012; Munch et al., 2014; Parker et al., 1971; Ross et al., 1965; Stein et al., 1966). It therefore seems that hyperthermia-induced tachycardia alone does not explain the augmented \dot{Q} because the concomitant shortened cardiac cycles and reduced cardiac filling time need to accommodate the increase in venous flow to the heart.

Central mechanisms such as increased intrathoracic pressure gradient induced by hyperventilation (i.e. the respiratory pump) and/or enhancement of the left ventricular (LV) systolic and diastolic functions (including diastolic suction; Nikolić et al., 1988) could at least in part mediate the hyperthermia-induced increased \dot{Q} . However, these factors might not have profound effects on \dot{Q} , as the hyperventilation (Fujii et al., 2015; Tsuji et al., 2019; White, 2006) and the enhanced LV functions (Stöhr, González-Alonso, Pearson et al., 2011) at rest are closely associated with the rise in core temperature. In this light, recent studies in humans reveals that single-leg (Koch Esteves et al., 2021), unilateral arm (Kalsi et al., 2017) and bilateral arm (van Mil et al., 2016) hyperthermia concurrently increase blood flow at the heated limb and \dot{Q} , despite no elevation in core temperature or any alterations in aerobic metabolism (Gibson et al., 2023). It has also been shown that changes in local vascular conductance are closely associated with local tissue and blood temperature (Chiesa et al., 2016; Kalsi et al.,

2017; Pearson et al., 2011), and that blood velocity and flow only increase in the conduit arteries perfusing the heated tissues within the leg (Koch Esteves et al., 2021, 2024). These observations point to localised heat-related increases in the peripheral perfusion, rather than central cardiorespiratory and metabolic factors, as an important influence on the hyperthermia-induced increase in \dot{Q} . To the best of our knowledge, however, the interplay between peripheral and central thermo-haemodynamic factors in the circulatory response to hyperthermia has not been fully established and understood.

A fundamental question is where the energy that accelerates the movement of blood with hyperthermia is derived from. According to Bernoulli's law, the total mechanical energy of blood is determined by the pressure energy generated by the heart, the gravitational potential energy and the kinetic energy of the flowing blood. Given the fact that the kinetic energy is proportional to the square of blood velocity, and that regional leg heating induces selective elevations in velocity and flow in the heated tissues (Koch Esteves et al., 2021, 2024), it is conceivable that heat energy, transferred in the periphery during thermal interventions, increases the kinetic energy of the flowing blood. The observation that blood velocity in the 3-day-old-chick embryo increases 3.7-fold with application of local infrared radiation even though the heart has been stopped supports this notion (Li & Pollack, 2023). A heat-dependent, vessel-based flow-driving mechanism may therefore accelerate blood flow to the heart, ultimately leading to an increase in systemic circulation (i.e. \dot{Q}). However, no study to date has explored the associations between heat-related changes in peripheral blood velocity or kinetic energy and the heart's output in humans. Answering this question will not only shed light on the longstanding debate of what drives blood circulation (Folkow & Neil, 1971; Furst, 2020; Furst & González-Alonso, 2024; Guyton, 1967; Joyce & Wang, 2021; Krogh, 1912a,b; Patterson & Starling, 1914; Rowell, 1993), but will also help establish the effectiveness of passive lower-limb heating as a therapeutic intervention to improve cardiovascular health.

Accordingly, the aim of this study was to comprehensively investigate the peripheral (leg, arm and head) and systemic circulatory, cardiorespiratory and metabolic responses to prolonged single-leg, two-leg and whole-body hyperthermia compared to a control normothermic condition. In addition, to shed light on the potential role of intrinsic and extrinsic cardiac factors on the central haemodynamic responses to hyperthermia, the impact of leg and whole-body hyperthermia on LV volumes along with LV mechanics, left intraventricular pressure gradients and ventriculo-arterial coupling were assessed. We hypothesised that the increase in \dot{Q} is closely related to the rise in peripheral haemodynamics across a wide range of hyperthermic conditions, and

that in opposition to the cardiocentric construct of blood circulation, central factors – such as alterations in the contributions of the respiratory pump, pressure propulsion and LV contractility and suction – are not obligatory for elevating \dot{Q} with hyperthermia.

Methods

Ethical approval

The study was approved by the Brunel University London Research Ethics Committee (6237-A-Jun/2017-7569-2) and was carried out in accordance with the *Declaration of Helsinki*. Written informed consent was obtained from all participants prior to commencement of the study.

Participants

Eight healthy males with a mean (\pm SD) age of 29 ± 11 years, height of 179 ± 7 cm and body mass of 73 ± 10 kg participated in the study. The participants were non-smokers and were not taking prescription medications.

Experimental design

Participants visited the laboratory on four occasions separated by >3 days, undergoing four randomly assigned and counterbalanced protocols: (1) 3 h of no heating (control); (2) 3 h of single-leg heating; (3) 3 h of two-leg heating; and (4) 2.5 h of whole-body heating. In comparison to the first three protocols, the whole-body heating trial was terminated earlier because all participants reached their limit of heat tolerance after 2.5 h. For all four protocols, participants were required to abstain from strenuous exercise and alcohol intake for 24 h and caffeine consumption for 12 h before the commencement of the protocol.

On the experimental day, participants arrived at the laboratory postprandial at 08.00 h, and body mass was measured after the voiding of urine. The participants then entered an environmental chamber set at 23°C and rested in a supine position on a bed. Following instrumentation and baseline measurements prior to heating, participants were fitted with a water-perfused garment on their right leg for protocol 2 (single-leg heating), both legs for protocol 3 (two-leg heating), and both legs and upper body except the head for protocol 4 (whole-body heating). The garment was connected to a thermostatically controlled water circulator (F-34, Julabo, Seelbach, Germany), which continuously circulated hot water (50°C outlet temperature exiting the water circulator system) and wrapped in a survival blanket to limit heat

loss. During the experimental protocols, LV volumes and functions and leg, arm and head haemodynamics were assessed every 30 min using an ultrasound system (see below for further details). Blood samples, respiratory and metabolic variables, and thermal sensation – an eleven-point scale, ranging from -5 (unbearably cold) to 5 (unbearably hot) with 0 being neutral, which is a scale slightly modified from that reported by Toner et al. (1986) – were also obtained at the same time points. HR, blood pressure and body temperatures were recorded continuously. Participants ingested fluids during the heating protocols to maintain a normal hydration status (i.e. 0.1 ± 0.2 , 0.3 ± 0.1 and 0.9 ± 0.1 L h^{-1} of water during single-leg, two-leg, and whole-body heating, respectively).

Cardiac function

LV volume and function. LV volume and function were assessed using an ultrasound system (Vivid 7 Dimension; GE Medical, Horton, Norway) equipped with a sector array probe (M4S) according to current guidelines (Lang et al., 2015). Every 30 min during the protocols, echocardiographic images of five consecutive cardiac cycles were obtained during 45° left lateral tilt of the bed. All cardiac data are presented as the average of three consecutive cardiac cycles. Care was taken to ensure that all ultrasound settings, including image depth and frame rates, were kept constant within participants. Apical four-chamber and two-chamber images were recorded, and end-diastolic volume (LVEDV), end-systolic volume (LVESV) and SV were analysed using the Simpson's biplane method and the manufacturer's software (EchoPAC PC version 203; GE Healthcare, Tokyo, Japan). \dot{Q} was calculated as the product of HR and SV. Systemic vascular conductance was calculated as $\dot{Q}/\text{mean arterial pressure (MAP)}$. LV ejection and filling times and isovolumetric contraction and relaxation times were assessed using pulsed wave tissue Doppler imaging of the septal mitral annular velocity (Alam et al., 1999; Stöhr, González-Alonso & Shave, 2011).

Systolic and diastolic LV mechanics. Systolic and diastolic LV mechanics were assessed from parasternal short-axis images recorded at the mitral valve and apical level as described in detail previously (Stöhr et al., 2016). In brief, images at the mitral valve level (basal level) were standardized by ensuring that the images were taken as cranially as possible and the full thickness of the myocardium was imaged throughout the cardiac cycle. Apical short-axis views were obtained by identifying the standardised apical four-chamber location, and then tilting the probe into the short-axis plane and keeping the

probe as close to the apex as possible, whilst ensuring a circular view without luminal obliteration at end-systole. A single focal point was positioned in the centre of the ventricular cavity for all short-axis images. Images were analysed off-line for two-dimensional speckle tracking-derived LV twist mechanics. From the raw speckle tracking output, data were interpolated to 600 points at equidistant time intervals in systole and diastole, respectively, as previously recommended (Burns et al., 2008). The frame-by-frame basal rotation ($^{\circ}$) and rotation velocity ($^{\circ} \text{ s}^{-1}$) data were subtracted from apical rotation and rotation velocity data, respectively, to determine peak systolic LV twist ($^{\circ}$) and early diastolic untwisting rate ($^{\circ} \text{ s}^{-1}$). Similarly, systolic radial and circumferential strain (both %) were quantified from speckle tracking analysis of parasternal short-axis images.

Intra-ventricular pressure gradients. Left intra-ventricular pressure gradients from the LV base to the apex in early diastole were quantified using a validated approach based on colour-Doppler M-mode images in the apical four-chamber view (Greenberg et al., 2001; Notomi et al., 2006; Rovner et al., 2003). The Doppler M-mode cursor was aligned with the diastolic inflow streamline and the images were analysed with an image processing algorithm based on the one-dimensional Euler equation. Peak left intraventricular pressure gradients were defined as the maximal pressure difference between the LV base (mitral annulus) and the LV apex.

Leg, arm and head haemodynamics

Blood flow was measured every 30 min during the protocols in the common femoral artery (CFA), brachial artery (BA), common carotid artery (CCA) and internal carotid artery (ICA) as previously described (Kalsi et al., 2017; Koch Esteves et al., 2021; Trangmar et al., 2014) using a 10 MHz linear probe (10L). The water-perfused garment had custom-made openings which allowed the probe to be placed on the skin with minimal heat loss. CFA blood flow measurements were acquired at a position 2–3 cm distal to the inguinal ligament in participants' right leg (i.e. the heated leg except in the control trial). For the measurement of BA blood flow, the participants' right arm was extended and positioned on a table at the side of the bed, and blood flow was obtained ~5 cm proximal to the antecubital fossa. The right CCA and ICA blood flow were measured ~1.5 cm proximal to and ~1.0–1.5 cm distal to the carotid bifurcation, respectively. Longitudinal images of the arteries were recorded when the intima-media boundary was clearly visible, and arterial diameters related to systole and diastole were measured as the largest and smallest diameters within each cardiac cycle.

Mean diameter was calculated as systolic diameter \times 1/3 + diastolic diameter \times 2/3. CFA, BA, CCA and ICA cross-sectional areas (CSAs; in cm^2) were estimated as follows: $\text{CSA} = \pi \times (\text{mean diameter}/2)^2$. Blood velocity was measured simultaneously with artery images using continuous pulsed-wave Doppler at a frequency of 4.4 MHz, with an insonation angle consistently below 60° and the sample volume extended to cover the entire vessel lumen. Continuous 12-s blood velocity profiles were recorded and analysed offline to calculate time-averaged mean blood velocity (V_{mean}) with the manufacturer's software (EchoPAC PC version 112; GE Medical, Horton, Norway). CFA, BA, CCA and ICA blood flow were calculated as the product of the V_{mean} (in cm s^{-1}) and CSA (in cm^2) and were multiplied by 60 and divided by 1000 to obtain values expressed in L min^{-1} . ICA blood flow was multiplied by 2 to calculate anterior cerebral blood flow, an index of brain blood flow which accounts for ~78% of the total cerebral blood flow (Bain et al., 2020; Gibbons et al., 2020, 2021; Ogoh et al., 2013). Additionally, external carotid artery (ECA) blood flow was calculated by subtracting ICA blood flow from CCA blood flow and then doubled to obtain extracranial blood flow. CFA, BA, CCA, ICA and ECA vascular conductance were calculated as the corresponding vessel blood flow/MAP. Assuming that the rate of arterial inflow and venous outflow are the same during steady-state condition, the volume of blood passing through the peripheral veins during each cardiac cycle (beat volume; in mL) was estimated by dividing blood flow in the CFA, BA and CCA by HR; they were then doubled and added together to obtain an index of the limbs and head beat volume during the control, the two-leg heating and the whole-body heating trials. During the single-leg heating trial, however, the legs' beat volume was estimated as the sum of the heated and control legs blood flows divided by HR, with the control (non-heated) leg blood flow being stable as in the control trial (Koch Esteves et al., 2021, 2023). To obtain mechanistic information on the forces driving blood circulation, kinetic energy (KE) of flowing blood in the limbs and head was calculated as follows: $\text{KE} (\text{mJ beat}^{-1}) = \frac{1}{2} \rho V v^2$ where ρ is blood density (assumed to be 1.0506 g mL^{-1} as previously reported by Trudnowski & Rico, 1974), V is blood volume (on a per beat basis: beat volume), and v is blood velocity (calculated as average blood velocity in the CFA, BA and CCA multiplied by duration of the cardiac cycle in s). Blood kinetic energy in brain was also estimated in the same way using anterior cerebral beat volume and blood velocity.

Haematological parameters

Blood samples were taken via a venous cannula inserted into a superficial antecubital vein for subsequent

measurements of haemoglobin (Hb) concentration via the azidemetoglobin method (HemoCue® Hb 201+ System, HemoCue AB, Ängelholm, Sweden) and haematocrit (Hct), measured in quadruplicate using standard sodium-heparinized capillary tubes (micro-haematocrit tubes, Hawksley, Lancing, UK) and centrifugation (5 min; HaematoSpin 1400, Hawksley) procedures. The percent changes in blood, red cell and plasma volumes were calculated from the Hb and Hct values as described by Dill and Costill (1974). The absolute changes in blood, red cell and plasma volumes (L) were then estimated using previously reported equations (Sawka et al., 1992). The placement of a venous catheter was not successful for one participant; therefore, blood samples were obtained in seven participants.

Heart rate, arterial pressure and body temperatures

HR was monitored via a three-lead electrocardiogram. Arterial blood pressure was measured non-invasively using finger photoplethysmography (Finometer, Finapres Medical Systems, Enschede, The Netherlands). The monitoring cuff was placed around the middle finger of the right hand, with the forearm and hand supported so that the cuff was positioned at the vertical level of the heart. Core temperature was assessed using a commercially available rectal probe (RET-1, Physitemp Instruments, Clifton, NJ, USA) inserted 15 cm past the sphincter muscle and connected to a thermocouple meter (TC-2000, Sable Systems, North Las Vegas, NV, USA). Skin temperature from six sites (forehead, chest, arm, thigh, calf and foot) was obtained using commercially available thermistors (IT-18, Physitemp Instruments). Mean skin temperature from four sites (chest, arm, thigh and calf) was calculated using a standard weighted formula (Ramanathan, 1964) and then mean body temperature from core and mean skin temperatures was obtained as previously described (Hardy et al., 1938). Mean leg skin temperature was calculated from three skin temperatures weighted to the following regional proportions: 63% thigh, 28% calf and 9% foot based on previously reported body segment weights (Plagenhoef et al., 1983). Muscle temperature in the vastus lateralis muscle of the right thigh was measured using a thermistor (T-204f, Physitemp Instruments) inserted via an 18G catheter ~3 cm into the mid-portion of the muscle. The temperature probe and thermistors were connected to a thermocouple meter (TC-2000, Sable Systems) with the data being sampled at 1000 Hz together with analogue signals of the electrocardiogram and blood pressure waveform using a data acquisition unit (Powerlab 16/30, ADInstruments, Bella Vista, NSW, Australia) and analysed off-line using a data analysis software (LabChart 8, ADInstruments).

Effective arterial elastance, LV end-systolic elastance, and ventriculo-arterial coupling

Effective arterial elastance is widely accepted to reflect the net arterial load imposed on the LV, whereas the LV end-systolic elastance is an integrated measure of LV performance (Sagawa et al., 1977; Sunagawa et al., 1983). To obtain additional information on the cardiac afterload and myocardial contractility, we calculated non-invasive indexes of effective arterial elastance ($0.9 \times$ systolic blood pressure/SV) and LV end-systolic elastance ($0.9 \times$ systolic blood pressure/LVESV), respectively (Chantler & Lakatta, 2012; Chantler, Lakatta et al., 2008). We also evaluated the interaction of the LV contractile function and the load opposed by the arterial system, termed ventriculo-arterial coupling, by dividing LV end-systolic elastance by effective arterial elastance.

Respiratory and metabolic parameters

Inspired and expired gases were analysed using a metabolic cart (Vyntus® CPX, CareFusion, Höchberg, Germany). The flow sensor was calibrated using a calibration syringe at a fixed volume of air. The O₂ and CO₂ sensors were calibrated with room air and reference gases of known concentration (O₂ 15%, CO₂ 5%, N₂ balance). Oxygen uptake (\dot{V}_{O_2}), carbon dioxide output (\dot{V}_{CO_2}), pulmonary ventilation (\dot{V}_E), tidal volume, respiratory frequency and end-tidal O₂ and CO₂ pressures (P_{ETO_2} and P_{ETCO_2} , respectively) were recorded on a breath-by-breath basis. Arterial O₂ content (C_{aO_2}) was calculated as: C_{aO_2} (mL L⁻¹) = $1.36 \times$ [Hb] \times arterial O₂ saturation + $0.03 \times P_{ETO_2}$ (assuming arterial O₂ saturation is 0.98 as previously shown by Chiesa et al., 2015; Pearson et al., 2011). Mixed venous O₂ content ($C_{\bar{v}O_2}$) was also calculated from \dot{V}_{O_2} , \dot{Q} and C_{aO_2} using the Fick equation ($C_{\bar{v}O_2} = C_{aO_2} - a\text{-}\bar{v} O_2$ difference where $a\text{-}\bar{v} O_2$ difference = \dot{V}_{O_2}/\dot{Q}).

Statistical analysis

Data are reported as means \pm SD unless otherwise stated. Differences in measured variables were assessed using a two-way repeated-measures analysis of variance (ANOVA) in which protocols (control, single-leg heating, two-leg heating and whole-body heating) and time (temperature data: baseline, 0, 0.5, 1, 1.5, 2, 2.5 and 3 h; the other data: baseline, 0.5, 1, 1.5, 2, 2.5 and 3 h) were the main factors. Bonferroni's method was used as a *post hoc* test. The relationships between selected physiological variables were evaluated using Pearson's product-moment correlation analysis. Statistical analyses were performed using IBM SPSS Statistics (version 28,

IBM Corp., Armonk, NY, USA). *P*-values of <0.05 were considered significant.

To assess relationships between circulatory and temperature responses, we performed regression analysis, and the linear, sigmoidal and exponential models were fitted using GraphPad Prism (version 8, GraphPad Software, San Diego, CA, USA) as previously reported (Foster et al., 2022; Koch Esteves et al., 2021). Akaike's information criterion was used to select the best regression model (Akaike, 1973). Where appropriate the curve fitting was conducted with the following (1) sigmoidal and (2) exponential models:

$$\text{Blood flow (L min}^{-1}\text{)} = \text{BF}_{\text{Bottom}} + \frac{\text{BF}_{\text{Top}} - \text{BF}_{\text{Bottom}}}{1 + \left(\frac{\text{BF50}}{x}\right)^{\text{HillSlope}}} \quad (1)$$

$$\text{Blood flow (L min}^{-1}\text{)} = \text{BF}_0 \cdot e^{k \cdot x} \quad (2)$$

where $\text{BF}_{\text{Bottom}}$ and BF_{Top} are minimum and maximum plateaus in the units of the blood flow respectively, x represents the input variable (i.e. local temperature), BF50 is the value of x that gives a response half way between the minimal and maximal responses of the blood flow, HillSlope is the steepness of the curve, BF_0 is the blood flow value when x (local temperature) is zero, and k is the rate constant. These parameters were calculated to find the optimal fit to the data (producing the least variance) according to the manufacturer's instructions.

Results

Hydration status, body temperature, and thermal sensation

Body mass and blood volume were similar among all trials (main effect of trial for body mass: $P = 0.909$; Table 1), except for the blood volume during the last hour of whole-body heating, which became lower compared with the control and single-leg heating trials ($\Delta = -286 \pm 260 \text{ mL vs. control, } P = 0.045, 0.020 \text{ and } 0.016 \text{ at } 1.5, 2 \text{ and } 2.5 \text{ h, respectively}$) in association with proportional reductions in plasma volume (Table 1). All temperatures remained unchanged during the control trial (Fig. 1). As per design, leg skin and thigh muscle (quadriceps) temperatures increased rapidly by 4–10°C in all heating trials, whereas core temperature increased gradually by $0.4 \pm 0.2, 0.7 \pm 0.2 \text{ and } 2.3 \pm 0.4^\circ\text{C}$ during single-leg, two-leg and whole-body heating, respectively (all $P < 0.001 \text{ vs. baseline at the end of the heating; Fig. 1}$). Arm skin temperature increased rapidly during whole-body heating ($P < 0.001 \text{ vs. baseline at } 0.5 \text{ h; Fig. 1}$) but not in the other trials ($P = 1.000 \text{ vs. baseline at } 0.5 \text{ h; Fig. 1}$), although it was elevated during the last hour of the two-leg

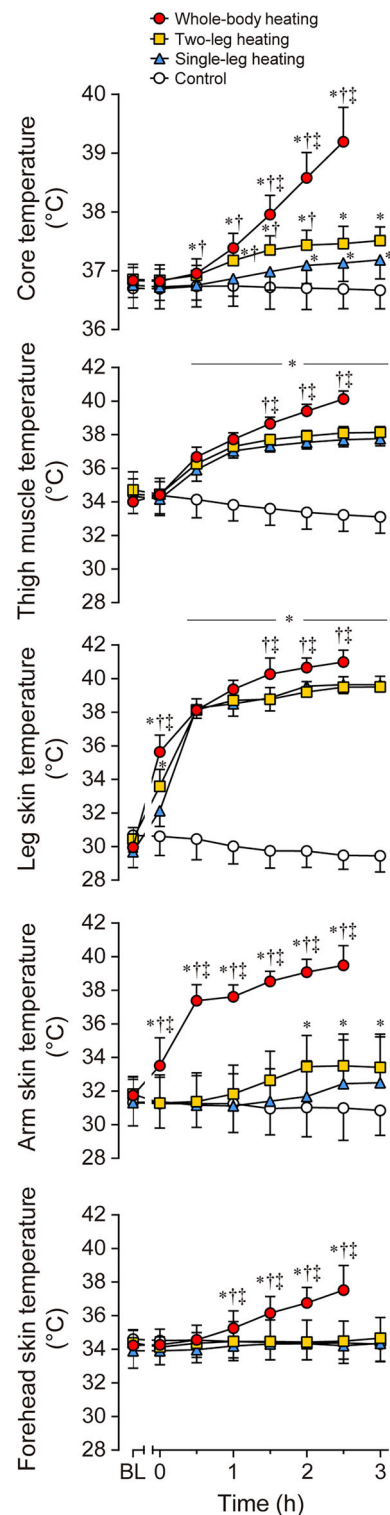


Figure 1. Core, thigh muscle (quadriceps) and regional skin temperatures during 3 h of no heating (control), single-leg heating and two-leg heating and 2.5 h of whole-body heating Data are means \pm SD for eight participants. BL signifies baseline measurements. * $P < 0.05 \text{ vs. control}$; † $P < 0.05 \text{ vs. single-leg heating}$; ‡ $P < 0.05 \text{ vs. two-leg heating}$. All variables below the horizontal line reported significant difference from control. [Colour figure can be viewed at wileyonlinelibrary.com]

Table 1. Body mass, blood parameters and thermal sensation

	Baseline	0.5 h	1 h	1.5 h	2 h	2.5 h	3 h
Body mass (kg)							
Control	72.5 ± 9.8	—	—	—	—	—	72.0 ± 10.0
Single-leg heating	72.3 ± 9.9	—	—	—	—	—	71.9 ± 9.9
Two-leg heating	72.5 ± 9.7	—	—	—	—	—	72.1 ± 9.8
Whole-body heating	72.2 ± 9.4	—	—	—	—	72.0 ± 9.5	—
Haemoglobin (g L⁻¹)							
Control	148 ± 14	150 ± 14	150 ± 14	150 ± 13	150 ± 13	150 ± 12	149 ± 12
Single-leg heating	147 ± 11	148 ± 12	147 ± 11	147 ± 10	148 ± 8	147 ± 7	150 ± 8
Two-leg heating	146 ± 9	148 ± 8	150 ± 9	150 ± 9	151 ± 7	151 ± 7	152 ± 8
Whole-body heating	148 ± 10	151 ± 12	155 ± 13	156 ± 14 [†]	159 ± 12 ^{*,†,‡}	159 ± 11 ^{*,†,‡}	—
Haematocrit (%)							
Control	46.6 ± 3.7	47.3 ± 4.1	47.4 ± 3.7	47.4 ± 3.5	47.7 ± 3.8	46.9 ± 4.0	46.8 ± 3.6
Single-leg heating	46.1 ± 1.7	46.4 ± 2.0	45.7 ± 2.1	46.0 ± 2.4	45.9 ± 2.4	46.3 ± 2.5	46.3 ± 2.6
Two-leg heating	46.1 ± 3.2	46.0 ± 2.8	46.0 ± 2.9	46.3 ± 3.0	46.5 ± 2.9	46.6 ± 2.9	46.9 ± 3.0
Whole-body heating	46.8 ± 3.9	46.4 ± 3.8	47.2 ± 4.2	48.0 ± 4.3	48.6 ± 4.1 [†]	48.6 ± 4.0	—
Red cell volume (L)							
Control	1.9 ± 0.2	1.9 ± 0.2	1.9 ± 0.2	1.9 ± 0.2	1.9 ± 0.2	1.9 ± 0.2	1.9 ± 0.2
Single-leg heating	1.9 ± 0.2	1.9 ± 0.2	1.9 ± 0.2	1.9 ± 0.2	1.9 ± 0.2	1.9 ± 0.2	1.9 ± 0.2
Two-leg heating	1.9 ± 0.2	1.9 ± 0.2	1.8 ± 0.2	1.8 ± 0.2	1.8 ± 0.2	1.8 ± 0.2	1.8 ± 0.2
Whole-body heating	1.9 ± 0.2	1.8 ± 0.2	1.8 ± 0.2	1.8 ± 0.2	1.8 ± 0.2	1.8 ± 0.2	1.8 ± 0.2
Plasma volume (L)							
Control	3.2 ± 0.3	3.1 ± 0.3	3.1 ± 0.3	3.1 ± 0.3	3.1 ± 0.3	3.1 ± 0.4	3.1 ± 0.3
Single-leg heating	3.2 ± 0.2	3.1 ± 0.3	3.2 ± 0.2	3.2 ± 0.3	3.1 ± 0.2	3.1 ± 0.2	3.1 ± 0.2
Two-leg heating	3.2 ± 0.2	3.1 ± 0.3	3.1 ± 0.2	3.1 ± 0.2	3.0 ± 0.3	3.0 ± 0.3	3.0 ± 0.2
Whole-body heating	3.2 ± 0.2	3.1 ± 0.2	3.0 ± 0.3 [†]	2.9 ± 0.3 [†]	2.8 ± 0.3 ^{*,†}	2.8 ± 0.3 [†]	—
Thermal sensation							
Control	-1.1 ± 0.4	-0.9 ± 0.7	-1.3 ± 0.7	-1.3 ± 0.7	-1.4 ± 0.9	-1.4 ± 1.2	-1.3 ± 1.0
Single-leg heating	-1.3 ± 0.7	0.1 ± 0.6	0.3 ± 0.5 [*]	0.4 ± 0.5 [*]	1.1 ± 0.7 [*]	1.3 ± 0.8 [*]	1.3 ± 0.7 [*]
Two-leg heating	-0.6 ± 0.5	1.6 ± 0.5 ^{*,†}	2.0 ± 0.9 ^{*,†}	2.8 ± 0.9 ^{*,†}	2.9 ± 0.6 ^{*,†}	2.8 ± 0.7 ^{*,†}	2.5 ± 0.9 [*]
Whole-body heating	-1.1 ± 1.1	2.5 ± 0.5 ^{*,†}	3.1 ± 0.6 ^{*,†}	3.4 ± 0.9 ^{*,†}	3.9 ± 0.9 ^{*,†}	4.2 ± 0.7 ^{*,†}	—

Data represented as mean ± SD. For body mass and thermal sensation, $n = 8$ participants; for blood parameters, $n = 7$ participants.

* $P < 0.05$ vs. control.

† $P < 0.05$ vs. single-leg heating.

‡ $P < 0.05$ vs. two-leg heating.

heating trial compared to control ($P = 0.015, 0.033$ and 0.027 at 2, 2.5 and 3 h, respectively, vs. control; Fig. 1). Forehead skin temperature remained unchanged in the control and both leg heating trials ($P = 0.449, 0.057$ and 1.000 vs. baseline at the end of the protocol in the control, single-leg heating and two-leg heating trials, respectively; Fig. 1), but increased gradually with whole-body heating ($P < 0.001$ vs. baseline at the end of heating; Fig. 1). The perceived thermal sensation remained unchanged in control (-1 , slightly cool; $P = 1.000$ vs. baseline at the end of the protocol; Table 1), but it increased in the heating trials in relation to the magnitude of heat stress, with values being perceived as 'slightly warm' (1) during single-leg heating, 'warm or hot' (2–3) during two-leg heating and 'very hot' (4) after 2.5 h of whole-body heating (all $P < 0.001$ vs. baseline at the end of the heating; Table 1).

Peripheral and systemic haemodynamics

Peripheral and systemic blood flow and blood pressure remained stable in control (Fig. 2). Leg blood flow increased progressively in all heating trials up to 0.5–0.9 L min⁻¹ above baseline (all $P < 0.001$ vs. baseline at 0.5 h; Fig. 2) whereas forearm blood flow increased during the two-leg and whole-body heating trials ($P < 0.006$ vs. control at the end of the heating; Fig. 2) and extracranial blood flow only increased during whole-body heating (0.27 ± 0.13 L min⁻¹; $P < 0.001$ vs. control at 2.5 h; Fig. 2). Conversely, anterior cerebral blood flow remained unchanged in all trials (main effect of trial, $P = 0.176$; time × trial interaction effect, $P = 0.130$; Fig. 2). The increases in leg, forearm and extracranial blood flow were solely or largely related to increases in blood velocity (leg: $\Delta = +3$ – 4 -fold vs. control, $P < 0.001$; forearm: $\Delta = +6$ – 12 -fold vs. control, $P < 0.001$; head:

$\Delta = +1.6$ -fold vs. control, $P < 0.001$), as vessel diameter remained unchanged in the CFA (main effect of trial, $P = 0.488$; time \times trial interaction effect, $P = 0.094$) or increased above control values in the BA and CCA (BA: $\Delta = +1.1$ – 1.3 -fold vs. control, $P < 0.007$; CCA: $\Delta = +1.1$ -fold vs. control, $P < 0.001$).

\dot{Q} increased gradually with single-leg, two-leg and whole-body heating ($\Delta = +2.1 \pm 0.6$, $+3.4 \pm 0.7$ and $+7.3 \pm 1.0$ L min⁻¹ vs. control, respectively, $P < 0.001$; Fig. 2) accompanied by increases in systemic vascular conductance ($\Delta = +28.3 \pm 8.3$, $+42.9 \pm 8.9$ and $+80.1$

± 15.8 mL min⁻¹ mmHg⁻¹ vs. control, respectively, $P < 0.001$; Fig. 2). MAP transiently decreased during the first hour of two-leg and whole-body heating ($\Delta = -10.9 \pm 8.2$ and -10.6 ± 6.5 mmHg vs. control, respectively, $P = 0.039$ and 0.011 at 0.5 h, 0.004 and 0.034 at 1 h, 0.018 and 1.000 at 1.5 h, 0.001 and 0.019 at 2 h; Fig. 2) but it returned gradually to the baseline levels and did not differ from control at the end of the heating ($P = 0.196$ and 1.000 in two-leg and whole-body heating, respectively; Fig. 2). Similar responses were observed in systolic arterial pressure (Fig. 2).

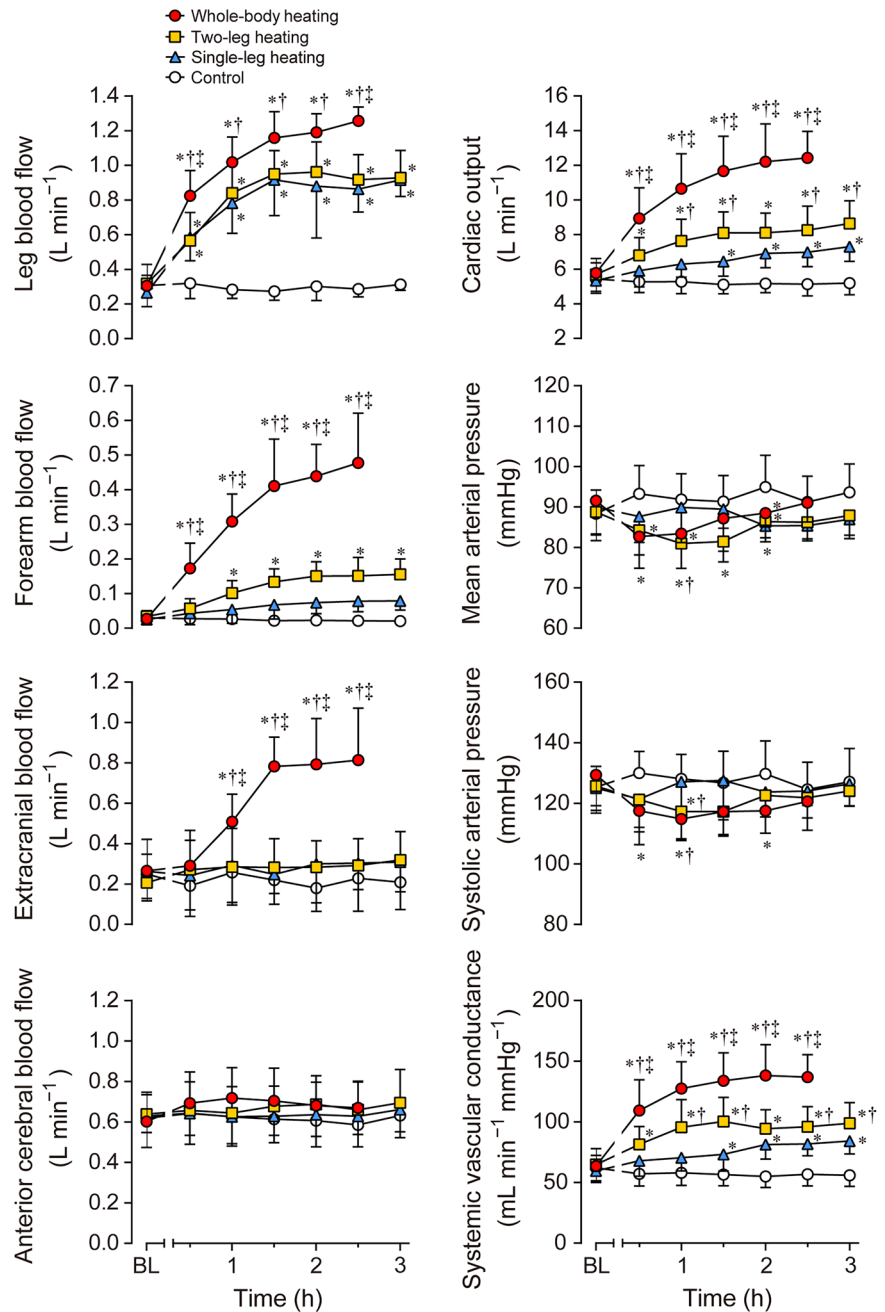


Figure 2. Peripheral and systemic haemodynamics during 3 h of no heating (control), single-leg heating and two-leg heating and 2.5 h of whole-body heating

Leg, forearm, extracranial and anterior cerebral blood flow indicate blood flows in the common femoral, brachial, bilateral external carotid and bilateral internal carotid arteries, respectively. Data are means \pm SD for 8 participants. BL signifies baseline measurements. * $P < 0.05$ vs. control; † $P < 0.05$ vs. single-leg heating; ‡ $P < 0.05$ vs. two-leg heating. [Colour figure can be viewed at wileyonlinelibrary.com]

LV volumes, heart rate, peripheral beat volume, intraventricular pressure gradients, blood kinetic energy, and LV ejection and filling times

LV volumes, peripheral beat volumes and blood kinetic energy, HR, filling and ejection times and early diastolic intraventricular pressure gradients of LV remained stable during control (Fig. 3). In all heating trials, SV increased compared to control ($\Delta = +23 \pm 12$ mL, $P < 0.003$ at the end of the heating in single-leg and two-leg heating and $P < 0.001$ in the first hour in whole-body heating; Fig. 3), but it returned to baseline levels after 1 h of whole-body

heating ($P = 0.429$ at 2.5 h; Fig. 3). The increased SV was associated with both enhanced LVEDV ($\Delta = +10 \pm 12$ mL vs. control, $P = 0.021$ at the end of the heating in two-leg heating and $P = 0.028$ at 0.5 h in whole-body heating; Fig. 3) and reduced LVESV ($\Delta = -12 \pm 5$ mL vs. control, $P < 0.007$ at the end of the heating in all heating trials; Fig. 3), but the subsequent return to baseline was solely related to a progressive decline in LVEDV to or slightly below control level ($\Delta = -10 \pm 15$ mL vs. control at 2.5 h, $P = 0.100$; Fig. 3), as LVESV decreased throughout heating ($\Delta = -17 \pm 7$ mL vs. control at 2.5 h, $P < 0.001$; Fig. 3). LV ejection fraction did not

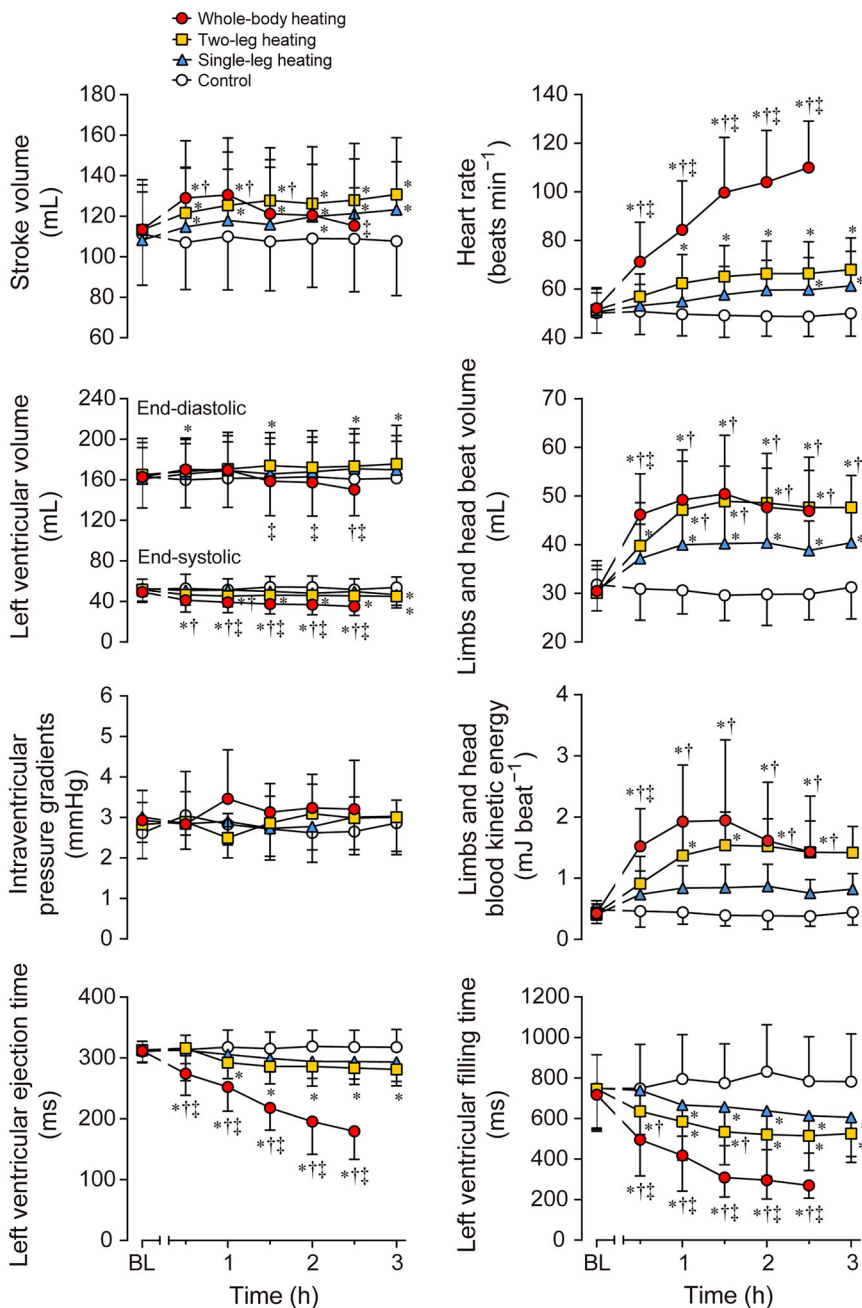


Figure 3. Stroke volume, heart rate, left ventricular (LV) volumes, peripheral beat volume, intraventricular pressure gradients, peripheral blood kinetic energy and LV ejection and filling times during 3 h of no heating (control), single-leg heating and two-leg heating and 2.5 h of whole-body heating

Cardiac images for intraventricular pressure gradients were successfully analysed in all data sets in seven participants and therefore the intraventricular pressure gradients data are from seven participants. The other parameters are from eight participants. Data are means \pm SD. BL signifies baseline measurements. * $P < 0.05$ vs. control; † $P < 0.05$ vs. single-leg heating; ‡ $P < 0.05$ vs. two-leg heating. [Colour figure can be viewed at wileyonlinelibrary.com]

change during control (66–68%; $P = 1.000$ vs. baseline) but increased 6–7% units in all the heating conditions compared to baseline (i.e. 73 ± 2 , 74 ± 3 and $77 \pm 3\%$ during single-leg, two-leg and whole-body heating at the end of the heating, $P < 0.001$ vs. control).

HR increased in all heating trials, but the magnitude of response was greater with whole-body compared to two-leg and single-leg heating ($\Delta = +61 \pm 13$, $+18 \pm 6$ and $+11 \pm 7$ beats min^{-1} , respectively, all $P < 0.008$ vs. control at the end of the heating; Fig. 3). The increase in HR was positively correlated to rise in core temperature ($R^2 = 0.891$, $P < 0.001$) and it increased 27 beats min^{-1} per 1°C rise in core temperature. The increases in HR were accompanied by a progressive shortening of LV ejection ($\Delta = -36 \pm 21$ and -139 ± 36 ms vs. control, respectively, $P < 0.008$ at the end of the heating; Fig. 3) and filling times ($\Delta = -257 \pm 129$ and -514 ± 170 ms vs. control, respectively, $P < 0.001$ at the end of the heating; Fig. 3) during two-leg and whole-body heating, whereas it was only related to a reduction in LV filling time during single-leg heating ($\Delta = -176 \pm 117$ ms vs. control, $P = 0.008$ at the end of the heating; Fig. 3). A similar response was observed in isovolumetric contraction ($\Delta = -33 \pm 18$ ms vs. control, $P < 0.039$ at the end of the heating in all the heating trials) and relaxation times ($\Delta = -27 \pm 11$ ms vs. control, $P < 0.022$ at 2 h in two-leg and whole-body heating). Limbs and head beat volume, an index of peripheral beat volume or HR-independent venous return, increased in all heating trials ($\Delta = +9 \pm 2$ to $+17 \pm 8$ mL vs. control, $P < 0.003$ at the end of the heating in all the heating trials; Fig. 3). The enhanced limbs and head blood kinetic energy was also observed with two-leg and whole-body heating ($\Delta = +1.0 \pm 0.3$ and $+1.1 \pm 0.8$ mJ beat^{-1} vs. control, respectively, $P < 0.002$ at the end of the heating; Fig. 3) whereas the intraventricular pressure gradients from the LV base to the apex remained stable in all trials (main effect of trial, $P = 0.300$; time \times trial interaction effect, $P = 0.693$; Fig. 3).

Effective arterial elastance, LV end-systolic elastance and ventriculo-arterial coupling

Elastance and ventriculo-arterial coupling remained stable in control (Fig. 4). Ventriculo-arterial coupling increased with whole-body heating from 0.5 h onward ($\Delta = +1.3 \pm 0.6$ arbitrary units vs. control, $P < 0.001$ at the end of the heating; Fig. 4), reflecting a rapid decrease in effective arterial elastance ($P < 0.003$ vs. control at 0.5–2 h; Fig. 4) and a progressive increase in LV end-systolic elastance ($P < 0.021$ vs. control at 1–2.5 h; Fig. 4). The enhanced ventriculo-arterial coupling was also observed with single-leg and two-leg heating ($\Delta = +0.7 \pm 0.3$ and $+1.0 \pm 0.5$ arbitrary unit vs. control, respectively, $P < 0.002$ at the end of the heating;

Fig. 4) but the response was slower (at 3 h and 1–3 h, respectively) and mainly reflected a reduced effective arterial elastance ($P = 0.019$ and 0.001 vs. control at 3 h, respectively; Fig. 4) as LV end-systolic elastance remained unchanged ($P = 0.250$ and 0.061 vs. control at 3 h, respectively; Fig. 4).

LV twist mechanics and strains

LV twist and LV untwisting rate remained stable in control and single-leg and two-leg heating trials (Fig. 5). However, LV twist increased with whole-body heating from 1 h onward ($\Delta = +12 \pm 5^\circ$ vs. control, $P = 0.001$, 0.013

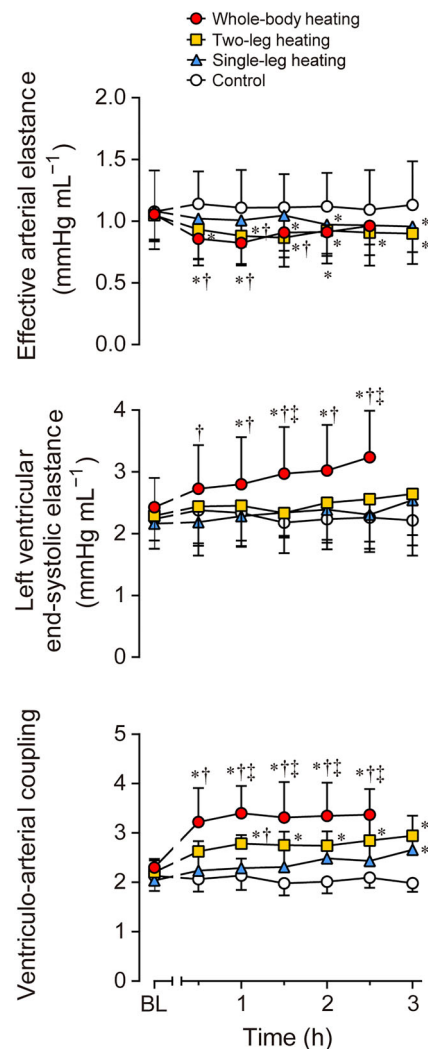


Figure 4. Effective arterial elastance, LV end-systolic elastance and ventriculo-arterial coupling during 3 h of no heating (control), single-leg heating and two-leg heating and 2.5 h of whole-body heating

Data are means \pm SD for eight participants. BL signifies baseline measurements. * $P < 0.05$ vs. control; † $P < 0.05$ vs. single-leg heating; ‡ $P < 0.05$ vs. two-leg heating. [Colour figure can be viewed at wileyonlinelibrary.com]

and <0.001 at 1, 1.5 and 2–2.5 h, respectively; Fig. 5), reflecting both enhanced basal rotation ($P = 0.004, 0.626$ and <0.001 at 1, 1.5 and 2–2.5 h, respectively; Table 2) and enhanced apical rotation ($P = 0.021, 0.266, 0.009$ and 0.007 at 1, 1.5, 2 and 2.5 h, respectively; Table 2). A similar pattern of response was observed in LV untwisting rate which only changed during whole-body heating ($\Delta = -100 \pm 71^\circ$ vs. control, $P = 0.014, 0.089, 0.004$ and 0.023 at 1, 1.5, 2 and 2.5 h, respectively; Fig. 5) and it was associated with both enhanced basal rotation rate ($P = 0.017, 0.164$ and <0.001 at 1, 1.5 and 2–2.5 h, respectively; Table 2) and enhanced apical rotation rate ($P = 0.001, 0.058, 0.012$ and 0.010 at 1, 1.5, 2 and 2.5 h, respectively; Table 2). Peak apical circumferential strain increased during whole-body heating from 0.5 to 2 h ($P = 0.043, 0.008, 0.005$ and 0.014 at 0.5, 1, 1.5 and 2 h, respectively; Table 2), whereas peak radial (basal: main effect of trial, $P = 0.234$; time \times trial interaction effect, $P = 0.063$; apical: main effect of trial, $P = 0.625$; time \times trial interaction effect, $P = 0.238$; Table 2) and basal circumferential strain (main effect of trial, $P = 0.305$; time \times trial interaction effect, $P = 0.211$; Table 2) remained unchanged in all trials.

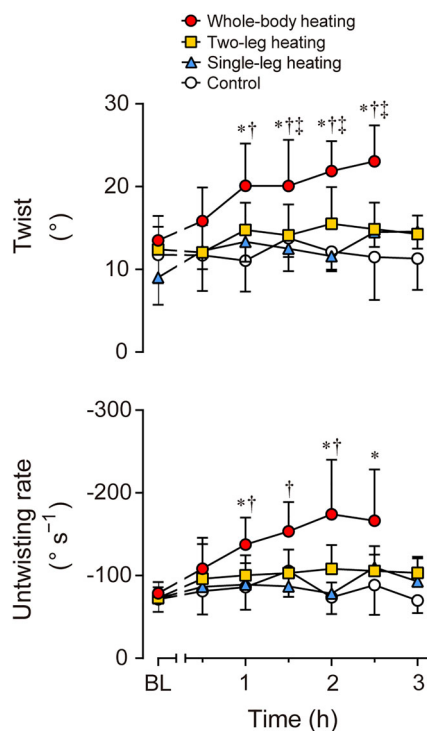


Figure 5. LV twist and untwisting rate during 3 h of no heating (control), single-leg heating and two-leg heating and 2.5 h of whole-body heating

Data are means \pm SD for six participants (cardiac images for LV twist mechanics were successfully analysed in all data sets in this number of participants). BL signifies baseline measurements. * $P < 0.05$ vs. control; † $P < 0.05$ vs. single-leg heating; ‡ $P < 0.05$ vs. two-leg heating. [Colour figure can be viewed at wileyonlinelibrary.com]

Metabolic, respiratory and blood responses

\dot{V}_{O_2} , \dot{V}_{CO_2} and \dot{V}_E remained unchanged in the control and the leg heating trials (Fig. 6), but they gradually increased during whole-body heating ($P < 0.001$ vs. baseline at the end of the heating; Fig. 6) such that \dot{V}_{O_2} , \dot{V}_{CO_2} and \dot{V}_E after

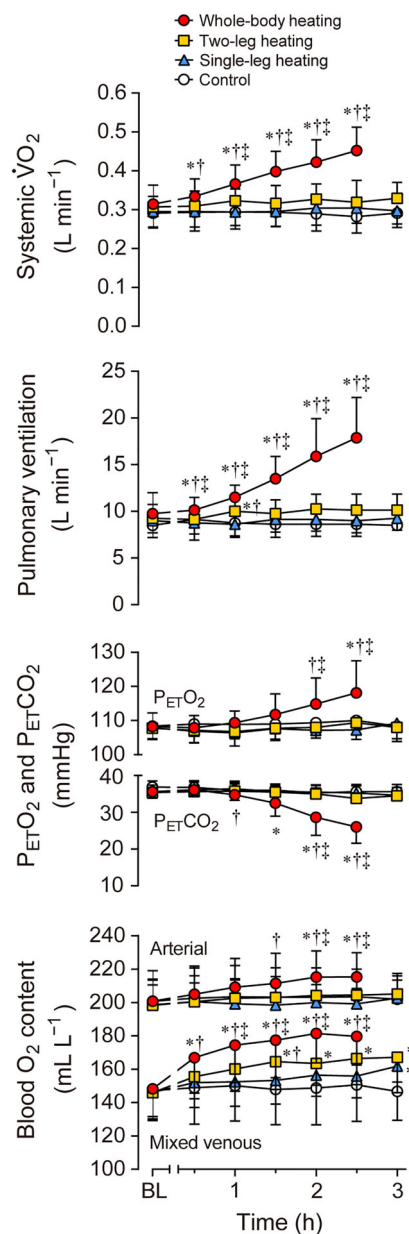


Figure 6. Systemic \dot{V}_{O_2} , pulmonary ventilation, end-tidal O_2 (P_{ETCO_2}) and CO_2 (P_{ETCO_2}) pressures and blood O_2 content during 3 h of no heating (control), single-leg heating and two-leg heating and 2.5 h of whole-body heating

Blood O_2 content data are from seven participants whereas the other parameters are from eight participants. Data are means \pm SD. BL signifies baseline measurements. * $P < 0.05$ vs. control; † $P < 0.05$ vs. single-leg heating; ‡ $P < 0.05$ vs. two-leg heating. [Colour figure can be viewed at wileyonlinelibrary.com]

Table 2. Peak systolic and diastolic LV rotation and strain parameters

	Baseline	0.5 h	1 h	1.5 h	2 h	2.5 h	3 h
Systolic component							
Basal rotation (°)							
Control	-2.4 ± 1.2	-3.1 ± 1.9	-2.7 ± 1.3	-3.3 ± 2.0	-3.1 ± 1.5	-2.3 ± 1.7	-2.6 ± 1.7
Single-leg heating	-2.3 ± 1.7	-3.7 ± 2.0	-4.4 ± 1.7	-4.0 ± 2.3	-4.1 ± 1.4	-4.0 ± 1.8	-4.1 ± 1.5
Two-leg heating	-3.9 ± 1.0	-3.5 ± 1.3	-4.7 ± 2.3	-5.1 ± 2.0	-4.5 ± 1.6	-5.1 ± 1.2	-5.7 ± 1.8*
Whole-body heating	-3.7 ± 1.3	-5.2 ± 2.3	-6.9 ± 2.3*	-5.9 ± 3.4	-7.9 ± 2.1*†‡	-8.5 ± 1.3*†‡	
Apical rotation (°)							
Control	10.0 ± 2.9	10.0 ± 3.5	9.2 ± 2.8	11.7 ± 3.6	10.6 ± 2.1	10.8 ± 3.9	10.7 ± 3.6
Single-leg heating	9.5 ± 2.2	9.6 ± 2.1	10.9 ± 2.7	9.8 ± 3.2	9.1 ± 1.8	11.5 ± 2.3	11.9 ± 2.6
Two-leg heating	10.0 ± 3.2	10.3 ± 4.0	11.1 ± 2.9	10.9 ± 3.1	12.4 ± 3.5	10.7 ± 4.0	9.8 ± 2.5
Whole-body heating	10.4 ± 3.2	11.9 ± 3.8	14.8 ± 5.4*	15.6 ± 6.5†	16.1 ± 5.0*†	15.9 ± 4.6*†‡	
Basal radial strain (%)							
Control	43.1 ± 20.2	47.9 ± 26.9	51.0 ± 21.6	50.0 ± 28.2	55.6 ± 35.1	56.6 ± 27.7	56.8 ± 25.0
Single-leg heating	43.8 ± 21.6	37.6 ± 22.1	52.1 ± 27.9	34.1 ± 6.6	36.9 ± 11.6	41.5 ± 17.0	49.4 ± 16.6
Two-leg heating	53.3 ± 19.6	50.3 ± 13.5	41.3 ± 24.9	52.6 ± 10.3	49.5 ± 25.6	45.6 ± 27.1	39.3 ± 7.4
Whole-body heating	52.9 ± 27.6	40.8 ± 18.4	48.4 ± 24.3	57.7 ± 24.9	31.4 ± 18.1	34.9 ± 17.1	
Apical radial strain (%)							
Control	45.0 ± 15.6	41.1 ± 20.5	45.5 ± 23.9	45.2 ± 25.4	41.8 ± 17.9	44.8 ± 18.0	37.7 ± 20.7
Single-leg heating	46.0 ± 16.0	53.4 ± 30.2	42.6 ± 12.6	37.7 ± 15.7	45.6 ± 23.0	43.9 ± 15.9	46.1 ± 12.8
Two-leg heating	42.1 ± 22.4	40.2 ± 25.1	47.6 ± 21.2	39.8 ± 21.8	37.7 ± 33.3	39.2 ± 19.8	38.0 ± 20.0
Whole-body heating	48.0 ± 23.8	44.8 ± 23.6	44.3 ± 14.5	40.9 ± 16.1	37.0 ± 19.8	43.1 ± 16.0	
Basal circumferential strain (%)							
Control	-12.7 ± 1.4	-13.6 ± 1.6	-12.7 ± 2.0	-13.1 ± 2.1	-13.9 ± 2.6	-13.3 ± 1.2	-13.6 ± 1.8
Single-leg heating	-11.8 ± 3.0	-11.0 ± 4.8	-11.7 ± 4.0	-13.5 ± 2.0	-13.7 ± 2.1	-13.8 ± 2.7	-13.6 ± 2.9
Two-leg heating	-11.7 ± 3.2	-13.3 ± 2.6	-13.0 ± 1.5	-14.6 ± 2.0	-13.9 ± 1.8	-14.0 ± 3.7	-13.1 ± 3.6
Whole-body heating	-12.9 ± 4.3	-13.2 ± 3.8	-15.9 ± 3.3	-15.0 ± 4.2	-14.6 ± 3.5	-14.7 ± 3.4	
Apical circumferential strain (%)							
Control	-16.9 ± 3.0	-20.0 ± 3.2	-19.5 ± 4.7	-20.9 ± 3.2	-20.2 ± 3.7	-20.3 ± 3.5	-19.7 ± 3.4
Single-leg heating	-18.6 ± 2.9	-19.8 ± 3.5	-21.3 ± 3.0	-20.1 ± 3.9	-20.8 ± 4.4	-21.7 ± 4.1	-22.9 ± 4.8
Two-leg heating	-19.2 ± 4.2	-21.0 ± 4.4	-21.7 ± 4.3	-21.4 ± 4.3	-21.8 ± 5.2	-21.7 ± 5.6	-21.2 ± 3.6
Whole-body heating	-19.8 ± 3.5	-23.6 ± 4.3*†	-24.3 ± 4.1*	-25.9 ± 5.6*†‡	-25.1 ± 5.7*†	-23.1 ± 4.5	
Diastolic component							
Basal rotation rate (° s⁻¹)							
Control	30.3 ± 5.5	36.8 ± 15.8	39.5 ± 15.2	47.0 ± 25.3	37.0 ± 15.4	38.0 ± 19.4	39.9 ± 14.3
Single-leg heating	35.5 ± 19.0	41.6 ± 24.9	49.7 ± 22.6	47.4 ± 23.2	53.9 ± 27.5	47.2 ± 19.7	47.9 ± 23.1
Two-leg heating	39.0 ± 18.3	53.5 ± 19.3	55.4 ± 13.2	52.5 ± 8.3	52.5 ± 13.8	53.5 ± 9.6	59.2 ± 15.1
Whole-body heating	44.8 ± 16.1	63.2 ± 16.5	65.2 ± 6.4*	75.6 ± 22.7	89.9 ± 4.5*†‡	90.1 ± 10.1*†‡	

(Continued)

Table 2. (Continued)

	Baseline	0.5 h	1 h	1.5 h	2 h	2.5 h	3 h
Apical rotation rate ($^{\circ} \text{ s}^{-1}$)							
Control	-60.6 ± 14.9	-63.2 ± 15.9	-57.3 ± 16.4	-75.1 ± 17.4	-67.0 ± 16.2	-74.8 ± 27.0	-65.9 ± 13.9
Single-leg heating	-54.2 ± 7.9	-58.8 ± 14.6	-71.3 ± 14.9	-68.9 ± 12.1	-66.6 ± 8.6	-77.8 ± 13.5	-81.9 ± 24.2
Two-leg heating	-69.7 ± 23.4	-75.3 ± 18.9	-93.0 ± 11.5*	-88.0 ± 19.2	-93.6 ± 34.4	-84.2 ± 17.8	-91.2 ± 30.3
Whole-body heating	-59.2 ± 10.0	-86.2 ± 29.0	-112.3 ± 36.3*†	-121.5 ± 56.6†	-128.3 ± 42.8*†	-133.7 ± 49.5*†‡	

Data represented as mean ± SD. For body mass and thermal sensation, $n = 8$ participants; for blood parameters, $n = 7$ participants.

* $P < 0.05$ vs. control.
† $P < 0.05$ vs. single-leg heating.
‡ $P < 0.05$ vs. two-leg heating.

2.5 h were $0.17 \pm 0.04 \text{ L min}^{-1}$ (61%), $0.14 \pm 0.05 \text{ L min}^{-1}$ (64%) and $9.3 \pm 4.5 \text{ L min}^{-1}$ (111%) higher than control ($P < 0.001$; Fig. 6). A similar pattern of response was observed in P_{ETO_2} , P_{ETCO_2} and C_{aO_2} content which only changed during whole-body heating ($P < 0.004$ vs. baseline at the end of the heating; Fig. 6). However, C_{vO_2} increased during all the heating trials ($P < 0.001$ vs. baseline at the end of the heating; Fig. 6), accompanying reductions in systemic $a-\bar{v} \text{ O}_2$ difference and oxygen extraction.

Relationships between circulatory and temperature responses and systemic and peripheral haemodynamics

In all trials, close sigmoidal relationships were observed between the increase in leg blood flow or extracranial tissues blood flow and the increase in the corresponding local temperature (leg: $R^2 = 0.979$ (non-linear regression), $P < 0.001$ (correlation analysis; the same applies below); extracranial: $R^2 = 0.956$ (non-linear regression), $P < 0.001$; Fig. 7), whereas the increase in forearm blood flow was exponentially related to the increase in local temperature ($R^2 = 0.926$ (non-linear regression), $P < 0.001$; Fig. 7). Similar relationships were also observed between the increase in each regional vascular conductance and the rise in the corresponding local temperature (leg: $R^2 = 0.972$ (non-linear regression), $P < 0.001$; forearm: $R^2 = 0.903$ (linear regression), $P < 0.001$; extracranial: $R^2 = 0.717$ (linear regression), $P < 0.001$). The increase in \dot{Q} was positively correlated to increases in limbs and head blood flow ($R^2 = 0.983$, $P < 0.001$; Fig. 8), vascular conductance ($R^2 = 0.972$, $P < 0.001$; Fig. 8), mean blood velocity ($R^2 = 0.991$, $P < 0.001$; Fig. 8) and blood kinetic energy ($R^2 = 0.803$, $P < 0.001$; Fig. 8). Positive correlations were also observed between the increase in \dot{Q} and elevation in each regional blood flow (leg: $R^2 = 0.776$, $P < 0.001$; forearm: $R^2 = 0.954$, $P < 0.001$; extracranial: $R^2 = 0.823$, $P < 0.001$), vascular conductance (leg: $R^2 = 0.754$, $P < 0.001$; forearm: $R^2 = 0.963$, $P < 0.001$; extracranial: $R^2 = 0.860$, $P < 0.001$), blood velocity (leg: $R^2 = 0.782$, $P < 0.001$; forearm: $R^2 = 0.988$, $P < 0.001$; head: $R^2 = 0.917$, $P < 0.001$) and blood kinetic energy (leg: $R^2 = 0.168$, $P = 0.034$; forearm: $R^2 = 0.883$, $P < 0.001$), with the exception of a negative correlation between the increase in \dot{Q} and the decrease in blood kinetic energy in head ($R^2 = 0.682$, $P < 0.001$).

Discussion

The main findings from the present study are five-fold. First, single-leg and two-leg hyperthermia induced elevations in leg and forearm blood flow and significant

increases in \dot{Q} and systemic vascular conductance without altering brain and extracranial blood flow, LV systolic and diastolic functions, MAP, \dot{V}_E , or aerobic metabolism. This suggests that increases in leg tissue temperature $\leq 38^\circ\text{C}$ did not activate central cardiorespiratory or metabolism-mediated mechanisms. Second, whole-body hyperthermia, however, further elevated leg and forearm blood flow, \dot{Q} and systemic vascular conductance compared to leg(s) hyperthermia and increased head (extracranial) blood flow, LV systolic and diastolic functions, \dot{V}_E and \dot{V}_{O_2} with minimal or no changes in MAP. Third, the elevated \dot{Q} with regional and

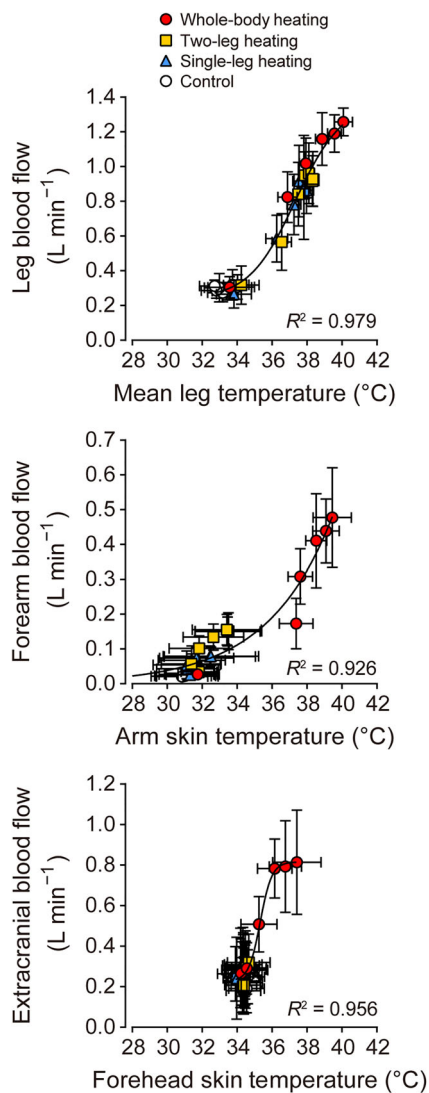


Figure 7. Relationships between circulatory and temperature responses during the control and heating trials

Sigmoidal and exponential models were applied in the relationships between the leg blood flow or extracranial blood flow and the local temperature and in the relationship between the forearm blood flow and the local temperature, respectively. Data are means \pm SD for eight participants. [Colour figure can be viewed at wileyonlinelibrary.com]

systemic hyperthermia was associated with proportional increases in systemic vascular conductance, related to elevations in blood flow, vascular conductance, blood velocity and blood kinetic energy in the limbs and head, but not in the brain. Fourth, at the cardiac level, the elevated \dot{Q} was associated with increased or maintained SV and an augmented HR. LVEDV was increased, unchanged or slightly reduced whereas LVESV was reduced in all heating trials. Elevations in peripheral (limbs and head) blood flow were primarily due to increases in blood velocity and accelerated blood supply to the heart, thereby contributing to the increased, maintained or slightly reduced LVEDV in spite of the shortened LV filling time. And lastly, fifth, the circulatory adjustments to leg and whole-body heating were met by an enhanced ventriculo-arterial coupling, reflecting over time reductions in net arterial load in all heating trials and an increased LV performance only with whole-body heating. Collectively, these results demonstrate distinct cardiorespiratory and metabolic responses to leg and whole-body hyperthermia but close coupling between limbs and head haemodynamics and \dot{Q} across a wide range of hyperthermic conditions. This suggests that central factors such as alterations in LV function and pressure propulsion forces related to cardiorespiratory and metabolic responses are not obligatory for increasing \dot{Q} during hyperthermia. Rather, local heat-related circulatory events selectively augmenting the velocity and kinetic energy of flowing blood appear to play an important role in the control of venous return and \dot{Q} during hyperthermia.

Factors controlling blood circulation with local and systemic hyperthermia

The key aim of this study was to establish the relationship between the peripheral and central haemodynamics across a wide range of hyperthermic states and gain insight into the underlying mechanisms. The comprehensive investigation of the time course of the peripheral and systemic circulatory, cardiorespiratory and metabolic responses to prolonged lower limb(s) and whole-body heating (compared to the appropriate normothermic control trial) provide new insight into the peripheral and central thermo-haemodynamic factors controlling blood circulation during hyperthermia. Of note is the finding that leg blood flow in all trials was tightly and proportionally related to the magnitude of increase in local limb temperature (Fig. 7). Similar positive relationships were observed in the forearm and in the head extracranial circulation (Fig. 7) with the increase in head perfusion only occurring when local temperature rose in the whole-body heating trial. How these hyperthermia-induced haemodynamic responses

may relate to \dot{Q} will be addressed below using Darcy's law of flow (the hydraulic equivalent of Ohm's law), the classic cardiac model where \dot{Q} is determined by intrinsic (i.e. contractility) and extrinsic (i.e. preload and afterload) factors and HR, and indices of pressure propulsion and suction forces generated by the heart. Six novel observations from the present study underscore the importance of the periphery in the control of \dot{Q} during hyperthermia.

First, the \dot{Q} response to single-leg, two-leg and whole-body hyperthermia (up to +2.1, +3.4 and +7.3 L min⁻¹ vs. control, respectively) was proportional to the increase in systemic as well as regional vascular conductance, as arterial pressure remained unchanged or was only transiently reduced across conditions. The classic cardiocentric postulate is that the heart is the primary organ generating the mechanical energy (pressure energy) to distribute systemic blood flow to organs and tissues

(Rowell, 1993; Secomb, 2016). This view has been termed the pressure-propulsion model (Furst, 2020; Furst & González-Alonso, 2024), and is exemplified by the close temporal relationship between the blood pressure and flow waves in the aorta (Khiri & Parker, 2005; Mynard et al., 2018; Parker & Jones, 1990) and the conduit arteries (Nichols et al., 2022). The observation that arterial, central venous and femoral venous pressures are maintained or only slightly altered (e.g. Crandall et al., 2008; Pearson et al., 2011; Rowell et al., 1969), however, indicates that the pressure propulsion forces remain essentially unchanged with increasing levels of passive hyperthermia. In support of this, a recent study found that the wave intensity-derived forward compression wave – which is generated during ventricular contraction and travels from the left ventricle to the peripheral vessels – remained unaffected by hyperthermia in the common femoral arteries of the heated and control legs

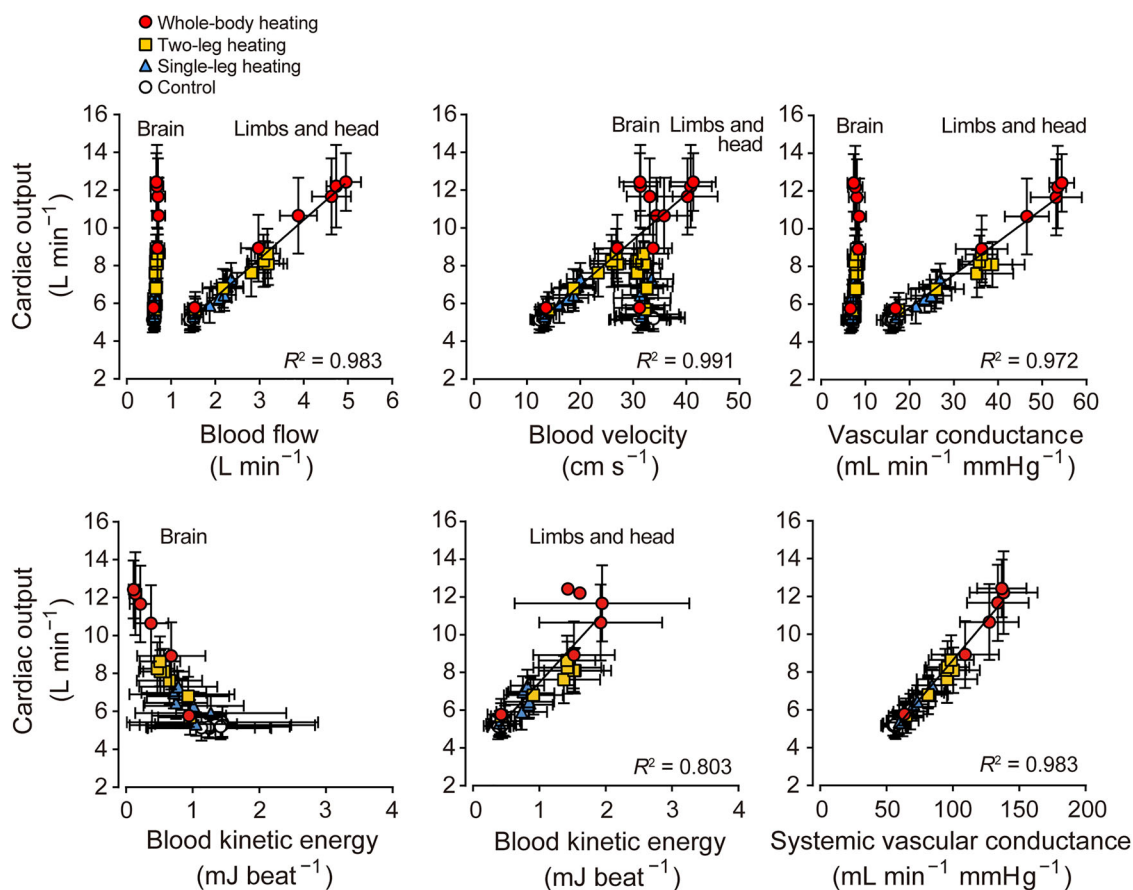


Figure 8. Relationships between systemic and peripheral haemodynamics during the control and heating trials

Limbs and head blood flow are total of bilateral flow in the common femoral, brachial, and common carotid arteries. Limbs and head vascular conductance were calculated in the same manner. Limbs and head blood velocity and kinetic energy are average blood velocity and kinetic energy of the common femoral, brachial, and common carotid arteries, respectively. Brain (anterior cerebral) blood flow and conductance are doubled values of blood flow in the internal carotid artery and the calculated conductance. Data are means \pm SD for eight participants. Lines are linear regression lines. [Colour figure can be viewed at wileyonlinelibrary.com]

during 3 h of unilateral leg heating, even though \dot{Q} increased and limb blood flow differed by several-fold during the heating intervention (Koch Esteves et al., 2021). It therefore appears that alterations in the pressure propulsion force generated by the heart do not explain the rise in peripheral and systemic blood flow during hyperthermia.

Second, single-leg and two-leg heating induced elevations in leg blood flow and significant increases in \dot{Q} and systemic vascular conductance without altering LV systolic and diastolic functions, ventilation, or systemic aerobic metabolism. According to the conventional cardiac model (Rowell, 1993), changes in intrinsic cardiac contractility and suction force affect \dot{Q} by altering LV volumes and pressure gradients. In this light, enhanced LV systolic and diastolic functions – as represented by increased systolic LV twist and diastolic LV untwisting rate, and an enhanced LV early diastolic intraventricular pressure gradients (indicative of LV sucking force) – could lead to more efficient ejection and filling (Beyar & Sideman, 1984; Notomi et al., 2006; Rovner et al., 2003; Yotti et al., 2005). It has also been demonstrated that deep breathing increases blood velocity in the venae cavae (Wexler et al., 1968), which is thought to facilitate cardiac filling and \dot{Q} via an increased intrathoracic pressure gradient (i.e. the respiratory pump) (Anholm et al., 1987). Lastly, metabolism-related mechanisms could impact \dot{Q} as indicated by the tight coupling between increases in limb and systemic blood flow and oxygen utilisation during exercise ($\sim 5\text{--}6\text{ L min}^{-1}$ per litre \dot{V}_{O_2} , e.g. González-Alonso et al., 2008; Mortensen et al., 2008). However, the significant increases in limb blood flow and \dot{Q} during single- and two-leg hyperthermia (up to $+1.2$ and $+3.4\text{ L min}^{-1}$, respectively) when LV function, diastolic suction force, ventilation and \dot{V}_{O_2} did not change, indicate that factors related to augmented myocardial function, hyperventilation and aerobic metabolism are not obligatory for the hyperthermia-induced increase in peripheral and systemic blood flow.

Third, anterior cerebral blood flow remained constant in the face of the large increase in \dot{Q} , which is in agreement with three human studies showing an unchanged anterior and total cerebral blood flow during graded whole-body hyperthermia (Bain et al., 2020; Gibbons et al., 2020, 2021), but is in contrast to the findings from two studies reporting reductions in anterior and total cerebral blood flow (Gibbons et al., 2021; Ogoh et al., 2013). Although splanchnic and renal blood flow were not measured, there is strong evidence that whole-body hyperthermia reduces perfusion in visceral organs (Minson et al., 1998; Rowell et al., 1970, 1971). Moreover, recent studies from our laboratory reveal that blood flow during segmental-leg hyperthermia only increases in the major conduit arteries (i.e. common, superficial and profunda femoral arteries and popliteal artery) and microcirculation perfusing the

heated tissues (Koch Esteves et al., 2021; 2024). This agrees with the present observation that blood flow in the common and external carotid arteries increased noticeably during whole-body heating, but not in the internal carotid artery despite the proximity of the measurement sites ($\sim 2\text{ cm}$). Together, this divergent circulatory response in the visceral organs and brain compared to the lower and upper extremities and in the heated and non-heated lower limb segments implies that the mechanisms regulating peripheral blood flow are not uniform among bodily sites, thus raising doubts over the general assumption that alterations in \dot{Q} determine the distribution of peripheral blood flow. If this assumption were correct, perfusion in all peripheral sites would increase when \dot{Q} is elevated.

Fourth, the increased or maintained SV in all the hyperthermic conditions was accompanied by a linear increase in HR closely related to the rise in core temperature (27 beats min^{-1} per 1°C). Should HR have been kept constant at baseline levels ($\sim 50\text{ beats min}^{-1}$), SV and LVEDV would have had to increase to $\sim 240\text{ mL}$ and $\sim 280\text{ mL}$ to account for the $\sim 12\text{ L min}^{-1}$ \dot{Q} during whole-body hyperthermia. The limited filling capacity of the human myocardium might appear to support the prevailing theory that core hyperthermia-mediated elevations in HR is the exclusive factor increasing \dot{Q} . Notwithstanding, the classic study of Knowlton & Starling (1912) demonstrated in the isolated mammalian heart that the rise in blood temperature increases HR but does not alter \dot{Q} because of the proportional reduction in SV. This agrees with human studies showing that raising HR through cardiac pacing reduces SV, resulting in the unchanged \dot{Q} and peripheral blood flow at rest and during exercise (Bada et al., 2012; Munch et al., 2014; Parker et al., 1971; Ross et al., 1965; Stein et al., 1966). Hence, an independent tachycardic response elicits shortenings of cardiac filling and ejection times which limit the ventricular filling and emptying, and thus reduce SV. This scenario contrasts with the presently observed increased or maintained LVEDV and reductions in LVESV in most or all of the hyperthermic conditions, which made it possible for SV to be elevated or maintained in the face of considerably shorter ventricular filling and ejection times (up to two-thirds and one-half, respectively; Fig. 3). Factors increasing venous flow to the heart are therefore crucial to augment \dot{Q} in conjunction with hyperthermia-induced tachycardia.

Fifth, estimates of venous beat volume in the limbs and head were enhanced by 30–60% in all hyperthermic conditions compared to control whereas similar estimates across the brain substantively decreased, especially during whole-body heating. The prospect of an enhanced net venous return and preserved cardiac filling in conditions of tachycardia is consistent with a study in anaesthetised mice demonstrating an increase in cross-sectional area

of inferior vena cava with hyperthermia (Crouch et al., 2018). Yet, some, but not all, human studies report that whole-body hyperthermia reduces indexes of cardiac preload such as right atrial pressure, central venous pressure and central blood volume (Crandall et al., 2008; Minson et al., 1998; Rowell et al., 1969). This is a phenomenon generally attributed to the shift of the blood volume from central to peripheral tissues and organs, possibly accentuated by the loss in circulating blood volume caused by the reduction in plasma volume as presently observed. Our direct LV volume data, however, revealed that cardiac preload was elevated or maintained in all hyperthermic conditions, implying appropriate blood volume mobilisation, venous return and cardiac filling, even in the face of diminished central venous pressure and/or blood volume during severe whole-body hyperthermia. This agrees with the observations that SV, Q and limb blood flow are maintained at rest and during exercise after withdrawal of 20% (~1.3 L) of blood volume (González-Alonso et al., 2006), which is much greater than the blood (plasma) volume losses seen in this study with severe whole-body hyperthermia.

And sixth, ventriculo-arterial coupling was enhanced in all heating trials owing to a reduced effective arterial elastance indicative of diminished net arterial load. Ventriculo-arterial coupling reflects the efficiency of energy transfer from the LV to the systemic circulation and is defined as the ratio of LV end-systolic elastance (an integrated measure of LV systolic performance) and effective arterial elastance (an index of the net arterial load imposed on the LV) (Hayashi et al., 2000; Starling, 1993). The interaction between the ventricle and arterial system could be altered by physiological stress. For example, ventriculo-arterial coupling has been shown to increase during exercise in humans, due to an augmented LV end-systolic elastance and a decrease or a small increase in effective arterial elastance (Asanoi et al., 1992; Chantler, Melenovsky et al., 2008; Najjar et al., 2004). During hyperthermia, however, changes in LV systolic performance seem to have a lesser effect on the ventriculo-arterial coupling because we found that LV end-systolic elastance only increased with whole-body hyperthermia. Of note, a study in isolated canine ventricles has demonstrated that effective arterial elastance – which is based on the three-element Windkessel model integrating the effects of peripheral vascular resistance, compliance, characteristic impedance and time of cardiac cycle – is largely dependent on the component of arterial resistance (or its inverse, arterial vascular conductance), which can have a major impact on SV (Sunagawa et al., 1983). In this light, increases in regional (leg, arm and head) as well as systemic vascular conductance were observed alongside the decreased net arterial load and enhanced LV ejection fraction. It therefore seems that peripheral mechanisms increasing ventriculo-arterial coupling and venous flow

to the heart had a positive effect on LV ejection and \dot{Q} during hyperthermia, with central factors including function of the heart and activities of respiratory and metabolic systems only playing an adjuvant role during whole-body hyperthermia (Fig. 9).

Thermosensitive mechanisms increasing blood circulation

In this study, arterial pressure declined only slightly and transiently during hyperthermia as previously discussed, and since the resting supine position was maintained throughout all the experimental protocols, it is likely that pressure and potential energies of flowing blood remained essentially unchanged. An important novel finding of this study is the significant increases in blood kinetic energy in the limbs and head in all hyperthermic conditions, but the opposite in the brain. The kinetic energy of flowing blood is estimated as $\frac{1}{2} \rho Vv^2$ (ρ : density; V : volume; v : velocity). In the present passive heating conditions, blood density (i.e. ρ) was unlikely to be altered considerably, whereas substantive increases in blood velocity in the limbs and head were observed during hyperthermia (Fig. 3). Although limbs and head beat volume (i.e. V) increased significantly, the kinetic energy is proportional to the square of velocity and increases in the square of the limbs and head blood velocity expressed per beat (v^2 ; up to +2.8-fold vs. control) were more pronounced than the rise in the V (up to +1.7-fold vs. control). The augmented blood velocity therefore largely explains the elevation in the kinetic energy of the flowing blood with hyperthermia. On entering the ventricles, blood velocity and hence kinetic energy fall virtually to zero (Wiggers, 1923). A kinetic energy gradient between the central veins and the ventricles therefore exists, which aids ventricular filling. The momentum of the returning blood from the periphery contributes to ventricular expansion and thus plays a role in the coupling of peripheral and central circulation. This interpretation is consistent with the observation in a recent human study showing that the increases in forearm blood flow and \dot{Q} during arm heating were prevented through partial arm blood flow restriction (van Mil et al., 2016), in line with the classic notion that the heart can only eject the blood it receives (Krogh, 1912a,b; Patterson & Starling, 1914). These findings suggest that the selective heat-induced acceleration in blood velocity is an important factor increasing blood kinetic energy and venous flow to the heart.

The presently observed positive relationships between blood flow and local temperature in the limbs and extracranial circulation raises the question of whether heat energy increases blood velocity and kinetic energy of the flowing blood indirectly by inducing vasodilatation and reductions in blood viscosity or directly via immediate

energy conversion. The unchanged or relatively small increase in conduit artery diameter, despite a substantial increase in the peripheral vascular conductance, suggests that the vasodilatation might have predominantly occurred in the downstream microvessels (e.g. small arteries and resistance arterioles). This idea is supported by previous findings of increased leg tissue oxygenation, indicative of an accelerated microcirculatory blood flow,

in association with elevated leg blood flow and vascular conductance during leg hyperthermia (Koch Esteves et al., 2021, 2023, 2024; Pearson et al., 2011). Considering that close associations exist between rise in temperature and erythrocyte-derived ATP release (Etulain et al., 2011; Kalsi & González-Alonso, 2012; Kalsi et al., 2017), and between increases in plasma ATP and limb blood flow (González-Alonso et al., 2015; Kalsi & González-Alonso,

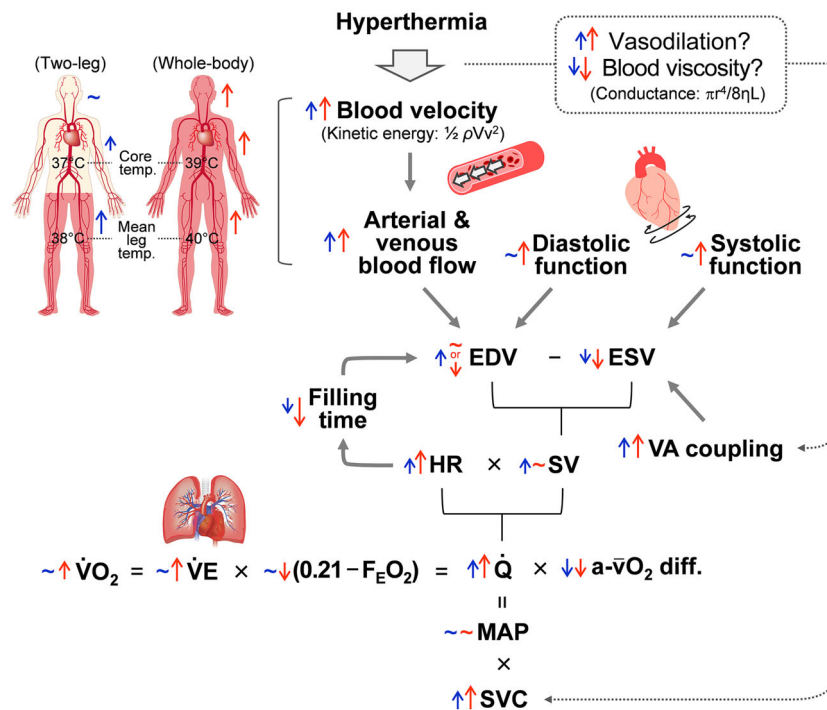


Figure 9. Schematic illustration of the impact of two-leg and whole-body hyperthermia on the circulatory system according to Darcy’s law of flow (the hydraulic equivalent of Ohm’s law) and Fick principle

Darcy’s law (the hydraulic equivalent of Ohm’s law) applied to the systemic circulation states that systemic flow (\dot{Q}) equals mean arterial pressure (MAP; assumed as perfusion pressure) times systemic vascular conductance (SVC). The Fick principle in turn states that oxygen consumption (\dot{V}_{O_2}) equals \dot{Q} times the arterial–venous oxygen content difference ($a\text{-}\bar{v} O_2$ diff.). On the other hand, \dot{V}_{O_2} is the product of pulmonary ventilation (\dot{V}_E) times the difference between inspiratory (0.21) and expiratory oxygen ($F_{E O_2}$) fractions. The responses after 2.5 h of the two-leg and whole-body heating interventions are compared. Two-leg hyperthermia (blue arrows) evoked elevations in leg and forearm blood flow and a significant increase in \dot{Q} and SVC; however, brain and extracranial blood flow, LV systolic and diastolic functions, \dot{V}_E , $P_{E T O_2}$, $P_{E T C O_2}$, \dot{V}_{O_2} , $\dot{V}_{C O_2}$ and MAP remained unchanged. In contrast, whole-body hyperthermia (red arrows) further elevated leg and forearm blood flow, \dot{Q} and SVC and enhanced LV systolic and diastolic functions, head (extracranial) blood flow, \dot{V}_E , $P_{E T O_2}$, $P_{E T C O_2}$, \dot{V}_{O_2} and $\dot{V}_{C O_2}$ without changing MAP or brain blood flow. Systemic \dot{V}_{O_2} was augmented in the face of a large reduction in $a\text{-}\bar{v} O_2$ diff. At the systemic level, the elevated \dot{Q} with leg and whole-body hyperthermia was associated with proportional increases in SVC, related to elevations in blood flow, vascular conductance, blood velocity and blood kinetic energy in the limbs and head, but not in the brain. At the cardiac level, the enhanced \dot{Q} was associated with an increased or maintained stroke volume (SV) and an augmented heart rate (HR). At the left ventricle (LV) level, LV end-diastolic volume (EDV) was increased, unchanged, or slightly reduced. This was accompanied by reduced LV end-systolic volume (ESV) and enhanced LV systolic function. Elevations in peripheral (limbs and head) blood flow primarily due to increases in blood velocity, accelerated blood velocity to the heart, thereby contributing to the increased or largely maintained EDV response despite the markedly shortened LV filling time. The circulatory adjustments to leg and whole-body heating were met by an enhanced ventriculo-arterial (VA) coupling, reflecting over time reductions in net arterial load in all heating trials and an increased LV performance only with whole-body heating. The distinct cardiorespiratory and metabolic responses to leg and whole-body hyperthermia but close thermo-haemodynamic coupling between periphery and \dot{Q} imply that local circulatory events altering the velocity and kinetic energy of the flowing blood influence the output of the heart during hyperthermia. [Colour figure can be viewed at wileyonlinelibrary.com]

2012; Kalsi et al., 2017; Pearson et al., 2011), it seems likely that red cell signalling-transduction mechanisms might be involved in the vasodilatory response in the micro-circulation. In addition to this, other biochemical signals released from the vascular endothelial cells such as nitric oxide (Kellogg et al., 1999; Minson et al., 2001) might also contribute to downstream vasodilation.

A different or complementary explanation is that alterations in blood's rheological properties are involved in the hyperthermia-induced increase in blood velocity and flow. This concept is in line with the findings from previous studies demonstrating that elevations in blood temperature are strongly associated with rises in red cell deformability and dispersion (Çinar et al., 2001; Manteuffel-Szoegé, 1960, 1969; Pinho et al., 2016) and reductions in blood viscosity and frictional resistance (Snyder, 1971; Çinar et al., 2001; Lim et al., 2010; Shin et al., 2004), although an increased blood viscosity has also been reported with acute whole-body hyperthermia in humans (Gibbons et al., 2020). Notably, an elegant study in the 3-day-old chick embryo model showed that when the heart was stopped, blood continued to flow, albeit at a lower velocity (Li & Pollack, 2023). Moreover, when infrared radiation was introduced, the *post mortem* blood velocity increased ~3.7-fold whereas blood slowed down when the infrared radiation was removed. The study also revealed that, on an intact chick embryo, blood failed to flow when the heat source that maintained a physiological body temperature was taken away. A heat-dependent, vessel-based flow-driving mechanism could therefore operate in the circulatory system (Li & Pollack, 2023; Manteuffel-Szoegé, 1960, 1969), working in synergy with the heart and the neurohumoral systems to increase flow and maintain the arterio-venous pressure gradients as generally observed in the present passive hyperthermia conditions. The observations in *ex vivo* pressurised preparations of small resistance arteries showing that temperature- and pharmacologically induced alterations in vascular tone can evoke substantial changes in blood flow in the absence of a heart are compatible with this notion (Duling & Berne, 1970; Ellsworth et al., 1995; Jones & Berne, 1964). These findings collectively support that local hyperthermia increases peripheral blood flow and vascular conductance selectively in the heated regions at least in part through the thermosensitive mechanisms inducing increases in blood velocity and kinetic energy of the flowing blood (Fig. 9). Whether this is mediated via microvessel vasodilatation, alterations in the blood's rheological properties and/or a direct effect of heat on blood kinetic energy awaits future investigation.

Limitations and methodological considerations

This study assessed the impact of prolonged hyperthermia on regional (leg, arm and head) vascular, cardio-

respiratory and metabolic responses across various hyperthermic conditions to gain insight into the control of the human circulation. We estimated the volume of blood passing through the peripheral (i.e. limbs and head) veins during each cardiac cycle (beat volume; in mL) as an index of venous return in the same manner as previous studies (Elstad et al., 2009; Trangmar & González-Alonso, 2017; Watanabe et al., 2020) based on an assumption that the rate of arterial inflow and venous outflow are the same during steady-state conditions. We did not measure cardiac function in the right side of the heart or pulmonary circulation; however, studies assessing both the right and left ventricular function and pulmonary haemodynamics show reciprocal functional changes to hyperthermic and/or exercise stress (Banks et al., 2010; Oxborough et al., 2011; Wilson et al., 2007). In this light, LVEDV tended to be lower during severe whole-body hyperthermia in the present study, similarly to right-sided preload as indexed by right atrial pressure and central venous pressure (Crandall et al., 2008; Minson et al., 1998; Rowell et al., 1969). In contrast, we found that cardiac preload evaluated by LVEDV was maintained or increased at any data points of leg(s) hyperthermia and mild to moderate (in the early and middle phase of) whole-body hyperthermia despite a markedly shortened LV filling time. Moreover, our peripheral beat volume data, which can reflect a dynamic property of venous return, imply that hyperthermia enhances venous blood mobilisation even in the condition of low cardiac preload on a pressure or volume basis (i.e. severe whole-body hyperthermia). Hence, although direct measurements of function of the right heart, pulmonary blood flow, or venous flow to the heart were not obtained in our study, the present data of LVEDV in relation to LV filling time derived using echocardiography strongly support our interpretation of the venous flow response during hyperthermia and our conclusion therefore remains intact. Lastly, we performed correlation analysis to gain insight into the interrelationship between the peripheral circulation and \dot{Q} , but these results do not demonstrate causality. In addition, the present study was conducted only on male participants. Future studies need to be conducted to conclusively establish whether there is a cause-and-effect relationship between the peripheral circulation and \dot{Q} , and to identify whether similar findings are observed in females and whether the phase of the menstrual cycle alters these responses.

Perspectives and significance

This study demonstrated profound and sustained increases in peripheral and central haemodynamics during the 2.5–3 h hyperthermia interventions. These haemodynamic responses are widely known to be strong stimuli for improving vascular health, and thus thermal

therapies (e.g. hot water baths, hot sand immersion or sauna) are recommended for patients with cardiovascular diseases, including chronic heart failure and peripheral artery disease (Brunt et al., 2016; Imamura et al., 2001; Kihara et al., 2002; Miyata & Tei, 2010; Shinsato et al., 2010). The applicability of these whole-body interventions to treat patients could, however, be limited by the fact that high elevations in core temperature are associated with systemic physiological strain and thermal discomfort. Notably, the present study revealed that the two-leg heating intervention can evoke sustained increases in lower limbs ($+1.2 \text{ L min}^{-1}$ assuming that the flows in both sides are same) and systemic ($+3.4 \text{ L min}^{-1}$) blood flow and reductions in net arterial load with a relatively small elevation in core temperature ($+0.4^\circ\text{C}$ compared to baseline), but without inducing thermal discomfort or stimulating a hyperventilatory response. These observations collectively support that prolonged lower limb heating could be an easily applicable and potentially effective intervention to improve cardiovascular health in individuals with low functional capacity.

Conclusions

The present findings demonstrate that the proportional increases in peripheral and central circulation with regional and systemic hyperthermia happen in the face of no changes in centrally generated pressure propulsion and suction forces, and no or minor changes in LV function and respiratory and metabolic activities. This suggests that these central factors and forces do not play an obligatory role in the increase in \dot{Q} during passive hyperthermia. Instead, the increases in \dot{Q} were closely related to the local heat-related rise in the velocity and kinetic energy of flowing blood in the limbs and head. Taken together, our findings highlight the importance of peripheral mechanisms in the control of the human blood circulation during hyperthermia, which have implications for the use of isolated and whole-body heat therapy to improve cardiovascular health in people with reduced functional capacity including those with circulatory diseases.

References

- Akaike, H. (1973). Information theory and an extension of the maximum likelihood principle. *Proceedings of the 2nd International Symposium on Information Theory, Akadémiai Kiadó, Budapest*, 267–281.
- Alam, M., Wardell, J., Andersson, E., Samad, B. A., & Nordlander, R. (1999). Characteristics of mitral and tricuspid annular velocities determined by pulsed wave Doppler tissue imaging in healthy subjects. *Journal of the American Society of Echocardiography*, **12**(8), 618–628.
- Anholm, J. D., Johnson, R. L., & Ramanathan, M. (1987). Changes in cardiac output during sustained maximal ventilation in humans. *Journal of Applied Physiology*, **63**(1), 181–187.
- Asanoi, H., Kameyama, T., Ishizaka, S., Miyagi, K., & Sasayama, S. (1992). Ventriculoarterial coupling during exercise in normal human subjects. *International Journal of Cardiology*, **36**(2), 177–186.
- Bada, A. A., Svendsen, J. H., Secher, N. H., Saltin, B., & Mortensen, S. P. (2012). Peripheral vasodilatation determines cardiac output in exercising humans: insight from atrial pacing. *The Journal of Physiology*, **590**(8), 2051–2060.
- Bain, A. R., Hoiland, R. L., Donnelly, J., Nowak-Flück, D., Sekhon, M., Tymko, M. M., Greiner, J. J., Desouza, C. A., & Ainslie, P. N. (2020). Cerebral metabolism, oxidation and inflammation in severe passive hyperthermia with and without respiratory alkalosis. *The Journal of Physiology*, **598**(5), 943–954.
- Banks, L., Sasson, Z., Busato, M., & Goodman, J. M. (2010). Impaired left and right ventricular function following prolonged exercise in young athletes: Influence of exercise intensity and responses to dobutamine stress. *Journal of Applied Physiology*, **108**(1), 112–119.
- Beyar, R., & Sideman, S. (1984). A computer study of the left ventricular performance based on fiber structure, sarcomere dynamics, and transmural electrical propagation velocity. *Circulation Research*, **55**(3), 358–375.
- Brunt, V. E., Howard, M. J., Francisco, M. A., Ely, B. R., & Minson, C. T. (2016). Passive heat therapy improves endothelial function, arterial stiffness and blood pressure in sedentary humans. *The Journal of Physiology*, **594**(18), 5329–5342.
- Burns, A. T., La Gerche, A., Prior, D. L., & Macisaac, A. I. (2008). Reduced and delayed untwisting of the left ventricle in patients with hypertension and left ventricular hypertrophy: A study using two-dimensional speckle tracking imaging. *European Heart Journal*, **29**(6), 825–826.
- Chantler, P. D., & Lakatta, E. G. (2012). Arterial-ventricular coupling with aging and disease. *Frontiers in Physiology*, **3**, 90.
- Chantler, P. D., Lakatta, E. G., & Najjar, S. S. (2008). Arterial-ventricular coupling: Mechanistic insights into cardiovascular performance at rest and during exercise. *Journal of Applied Physiology*, **105**(4), 1342–1351.
- Chantler, P. D., Melenovsky, V., Schulman, S. P., Gerstenblith, G., Becker, L. C., Ferrucci, L., Fleg, J. L., Lakatta, E. G., & Najjar, S. S. (2008). The sex-specific impact of systolic hypertension and systolic blood pressure on arterial-ventricular coupling at rest and during exercise. *American Journal of Physiology-Heart and Circulatory Physiology*, **295**(1), H145–H153.
- Chiesa, S. T., Trangmar, S. J., & González-Alonso, J. (2016). Temperature and blood flow distribution in the human leg during passive heat stress. *Journal of Applied Physiology*, **120**(9), 1047–1058.
- Chiesa, S. T., Trangmar, S. J., Kalsi, K. K., Rakobowchuk, M., Banker, D. S., Lotlikar, M. D., Ali, L., & González-Alonso, J. (2015). Local temperature-sensitive mechanisms are important mediators of limb tissue hyperemia in the heat-stressed human at rest and during small muscle mass exercise. *American Journal of Physiology-Heart and Circulatory Physiology*, **309**(2), H369–H380.

- Chiesa, S. T., Trangmar, S. J., Watanabe, K., & González-Alonso, J. (2019). Integrative human cardiovascular responses to hyperthermia. In *Heat stress in sport and exercise: Thermophysiology of health and performance*, In J. D. Périard & S. Racinais (Eds.), Springer, pp. 45–65.
- Çinar, Y. (2001). Blood viscosity and blood pressure: Role of temperature and hyperglycemia. *American Journal of Hypertension*, **14**(5), 433–438.
- Crandall, C. G., Wilson, T. E., Marving, J., Vogelsang, T. W., Kjaer, A., Hesse, B., & Secher, N. H. (2008). Effects of passive heating on central blood volume and ventricular dimensions in humans. *The Journal of Physiology*, **586**(1), 293–301.
- Crouch, A. C., Scheven, U. M., & Greve, J. M. (2018). Cross-sectional areas of deep/core veins are smaller at lower core body temperatures. *Physiological Reports*, **6**(16), e13839.
- Dill, D. B., & Costill, D. L. (1974). Calculation of percentage changes in volumes of blood, plasma, and red cells in dehydration. *Journal of Applied Physiology*, **37**(2), 247–248.
- Duling, B. R., & Berne, R. M. (1970) Propagated vasodilation in the microcirculation of the hamster cheek pouch. *Circulation Research*, **26**(2), 163–170.
- Ellsworth, M. L., Forrester, T., Ellis, C. G., & Dietrich, H. H. (1995). The erythrocyte as a regulator of vascular tone. *American Journal of Physiology-Heart and Circulatory Physiology*, **269**(6), H2155–H2161.
- Elstad, M., Nådland, I. H., Toska, K., & Walløe, L. (2009). Stroke volume decreases during mild dynamic and static exercise in supine humans. *Acta Physiologica*, **195**(2), 289–300.
- Etulain, J., Laponi, M. J., Patrucchi, S. J., Romaniuk, M. A., Benzaón, R., Klement, G. L., Negroto, S., & Schattner, M. (2011). Hyperthermia inhibits platelet hemostatic functions and selectively regulates the release of alpha-granule proteins. *Journal of Thrombosis and Haemostasis*, **9**(8), 1562–1571.
- Folkow, B., & Neil, E. (1971). *Circulation*. Oxford Univ. Press.
- Foster, J., Smallcombe, J. W., Hodder, S., Jay, O., Flouris, A. D., Nybo, L., & Havenith, G. (2022). Quantifying the impact of heat on human physical work capacity; part III: The impact of solar radiation varies with air temperature, humidity, and clothing coverage. *International Journal of Biometeorology*, **66**(1), 175–188.
- Fujii, N., Tsuji, B., Honda, Y., Kondo, N., & Nishiyasu, T. (2015). Effect of short-term exercise-heat acclimation on ventilatory and cerebral blood flow responses to passive heating at rest in humans. *Journal of Applied Physiology*, **119**(5), 435–444.
- Furst, B. (2020). *The heart and circulation: An integrative model*. Springer Nature Switzerland AG.
- Furst, B., & González-Alonso, J. (2024). The heart, a secondary organ in the control of blood circulation. *Experimental Physiology*. Advance online publication. <https://doi.org/10.1113/EP091387>
- Gibbons, T. D., Ainslie, P. N., Thomas, K. N., Wilson, L. C., Akerman, A. P., Donnelly, J., Campbell, H. A., & Cotter, J. D. (2021). Influence of the mode of heating on cerebral blood flow, non-invasive intracranial pressure and thermal tolerance in humans. *The Journal of Physiology*, **599**(7), 1977–1996.
- Gibbons, T. D., Tymko, M. M., Thomas, K. N., Wilson, L. C., Stembridge, M., Caldwell, H. G., Howe, C. A., Hoiland, R. L., Akerman, A. P., Dawkins, T. G., Patrician, A., Coombs, G. B., Gasho, C., Stacey, B. S., Ainslie, P. N., & Cotter, J. D. (2020). Global REACH 2018: The influence of acute and chronic hypoxia on cerebral haemodynamics and related functional outcomes during cold and heat stress. *The Journal of Physiology*, **598**(2), 265–284.
- Gibson, O. R., Astin, R., Puthuchery, Z., Yadav, S., Preston, S., Gavins, F. N. E., & González-Alonso, J. (2023). Skeletal muscle angiogenic, regulatory and heat shock protein responses to prolonged passive hyperthermia of the human lower limb. *American Journal of Physiology-Regulatory, Integrative and Comparative Physiology*, **324**(1), R1–R14.
- González-Alonso, J., Calbet, J. A. L., Boushel, R., Helge, J. W., Søndergaard, H., Munch-Andersen, T., Van Hall, G., Mortensen, S. P., & Secher, N. H. (2015). Blood temperature and perfusion to exercising and non-exercising human limbs. *Experimental Physiology*, **100**(10), 1118–1131.
- González-Alonso, J., Mortensen, S. P., Dawson, E. A., Secher, N. H., & Damsgaard, R. (2006). Erythrocytes and the regulation of human skeletal muscle blood flow and oxygen delivery: role of erythrocyte count and oxygenation state of haemoglobin. *The Journal of Physiology*, **572**(1), 295–305.
- González-Alonso, J., Mortensen, S. P., Jeppesen, T. D., Ali, L., Barker, H., Damsgaard, R., Secher, N. H., Dawson, E. A., & Dufour, S. P. (2008). Haemodynamic responses to exercise, ATP infusion and thigh compression in humans: Insight into the role of muscle mechanisms on cardiovascular function. *The Journal of Physiology*, **586**(9), 2405–2417.
- Greenberg, N. L., Vandervoort, P. M., Firstenberg, M. S., Garcia, M. J., & Thomas, J. D. (2001). Estimation of diastolic intraventricular pressure gradients by Doppler M-mode echocardiography. *American Journal of Physiology-Heart and Circulatory Physiology*, **280**(6), H2507–H2515.
- Guyton, A. C. (1967). Regulation of cardiac output. *New England Journal of Medicine*, **277**(15), 805–812.
- Hardy, J. D., Du Bois, E. F., & Soderstrom, G. F. (1938). Basal metabolism, radiation, convection and vaporization at temperatures of 22 to 35°C. *Journal of Nutrition*, **15**(5), 477–497.
- Hayashi, K., Shigemi, K., Shishido, T., Sugimachi, M., & Sunagawa, K. (2000). Single-beat estimation of ventricular end-systolic elastance-effective arterial elastance as an index of ventricular mechanoenergetic performance. *Anesthesiology*, **92**(6), 1769–1776.
- Imamura, M., Biro, S., Kihara, T., Yoshifuku, S., Takasaki, K., Otsuji, Y., Minagoe, S., Toyama, Y., & Tei, C. (2001). Repeated thermal therapy improves impaired vascular endothelial function in patients with coronary risk factors. *Journal of the American College of Cardiology*, **38**(4), 1083–1088.
- Jones, R. D., & Berne, R. M. (1964). Intrinsic regulation of skeletal muscle blood flow. *Circulation Research*, **14**(2), 126–138.
- Joyce, W., & Wang, T. (2021). How cardiac output is regulated: August Krogh's proto-Guytonian understanding of the importance of venous return. *Comparative Biochemistry and Physiology-Part A, Molecular & Integrative Physiology*, **253**, 110861.

- Kalsi, K. K., Chiesa, S. T., Trangmar, S. J., Ali, L., Lotlikar, M. D., & González-Alonso, J. (2017). Mechanisms for the control of local tissue blood flow during thermal interventions: Influence of temperature-dependent ATP release from human blood and endothelial cells. *Experimental Physiology*, **102**(2), 228–244.
- Kalsi, K. K., & González-Alonso, J. (2012). Temperature-dependent release of ATP from human erythrocytes: Mechanism for the control of local tissue perfusion. *Experimental Physiology*, **97**(3), 419–432.
- Kellogg, D. L., Liu, Y., Kosiba, I. F., & O'Donnell, D. (1999). Role of nitric oxide in the vascular effects of local warming of the skin in humans. *Journal of Applied Physiology*, **86**(4), 1185–1190.
- Khair, A. W., & Parker, K. H. (2005). Wave intensity in the ascending aorta: Effects of arterial occlusion. *Journal of Biomechanics*, **38**(4), 647–655.
- Kihara, T., Biro, S., Imamura, M., Yoshifuku, S., Takasaki, K., Ikeda, Y., Otuji, Y., Minagoe, S., Toyama, Y., & Tei, C. (2002). Repeated sauna treatment improves vascular endothelial and cardiac function in patients with chronic heart failure. *Journal of the American College of Cardiology*, **39**(5), 754–759.
- Knowlton, F. P., & Starling, E. H. (1912). The influence of variations in temperature and blood-pressure on the performance of the isolated mammalian heart. *The Journal of Physiology*, **44**(3), 206–219.
- Koch Esteves, N., Gibson, O. R., Khir, A. W., & González-Alonso, J. (2021). Regional thermal hyperemia in the human leg: Evidence of the importance of thermo-sensitive mechanisms in the control of the peripheral circulation. *Physiological Reports*, **9**(15), e14953.
- Koch Esteves, N., Khir, A. W., & González-Alonso, J. (2023). Lower limb hyperthermia augments functional hyperaemia during small muscle mass exercise similarly in trained elderly and young humans. *Experimental Physiology*, **108**(9), 1154–1171.
- Koch Esteves, N., McDonald, J., & González-Alonso, J. (2024). Thermo-haemodynamic coupling during regional thigh heating: Insight into the importance of local thermo-sensitive mechanisms on blood circulation. *Experimental Physiology*, **109**(4), 600–613.
- Krogh, A. (1912a). On the influence of the venous supply upon the output of the heart¹. *Skandinavisches Archiv Für Physiologie*, **27**(2), 126–140.
- Krogh, A. (1912b). The regulation of the supply of blood to the right heart. *Skandinavisches Archiv Für Physiologie*, **27**(2), 227–248.
- Lang, R. M., Badano, L. P., Mor-Avi, V., Afilalo, J., Armstrong, A., Ernande, L., Flachskampf, F. A., Foster, E., Goldstein, S. A., Kuznetsova, T., Lancellotti, P., Muraru, D., Picard, M. H., Rietzschel, E. R., Rudski, L., Spencer, K. T., Tsang, W., & Voigt, J.-U. (2015). Recommendations for cardiac chamber quantification by echocardiography in adults: An update from the American Society of Echocardiography and the European Association of Cardiovascular Imaging. *Journal of the American Society of Echocardiography*, **28**(1), 1–39.
- Li, Z., & Pollack, G. H. (2023). On the driver of blood circulation beyond the heart. *PLoS One*, **18**(10), e0289652.
- Lim, H.-J., Lee, Y.-J., Nam, J.-H., Chung, S., & Shin, S. (2010). Temperature-dependent threshold shear stress of red blood cell aggregation. *Journal of Biomechanics*, **43**(3), 546–550.
- Manteuffel-Szoegge, L. (1960). Energy sources of blood circulation and the mechanical action of the heart. *Thorax*, **15**(1), 47–53.
- Manteuffel-Szoegge, L. (1969). On the movement of the blood: The specific haemodynamic properties of the blood. *British Homoeopathic Journal*, **58**(03), 196–211.
- Minson, C. T., Berry, L. T., & Joyner, M. J. (2001). Nitric oxide and neurally mediated regulation of skin blood flow during local heating. *Journal of Applied Physiology*, **91**(4), 1619–1626.
- Minson, C. T., Wladkowski, S. L., Cardell, A. F., Pawelczyk, J. A., & Kenney, W. L. (1998). Age alters the cardiovascular response to direct passive heating. *Journal of Applied Physiology*, **84**(4), 1323–1332.
- Miyata, M., & Tei, C. (2010). Waon therapy for cardiovascular disease: Innovative therapy for the 21st century. *Circulation Journal*, **74**(4), 617–621.
- Mortensen, S. P., Damsgaard, R., Dawson, E. A., Secher, N. H., & González-Alonso, J. (2008). Restrictions in systemic and locomotor skeletal muscle perfusion, oxygen supply and VO₂ during high-intensity whole-body exercise in humans. *The Journal of Physiology*, **586**(10), 2621–2635.
- Munch, G. D. W., Svendsen, J. H., Damsgaard, R., Secher, N. H., González-Alonso, J., & Mortensen, S. P. (2014). Maximal heart rate does not limit cardiovascular capacity in healthy humans: Insight from right atrial pacing during maximal exercise. *The Journal of Physiology*, **592**(2), 377–390.
- Mynard, J. P., Penny, D. J., & Smolich, J. J. (2018). Major influence of a 'smoke and mirrors' effect caused by wave reflection on early diastolic coronary arterial wave intensity. *The Journal of Physiology*, **596**(6), 993–1017.
- Najjar, S. S., Schulman, S. P., Gerstenblith, G., Fleg, J. L., Kass, D. A., O'connor, F., Becker, L. C., & Lakatta, E. G. (2004). Age and gender affect ventricular-vascular coupling during aerobic exercise. *Journal of the American College of Cardiology*, **44**(3), 611–617.
- Nichols, W. W., O'Rourke, M., Edelman, E. R., & Vlachopoulos, C. (2022). *McDonald's blood flow in arteries: Theoretical, experimental and clinical principles*. CRC Press.
- Nikolić, S., Yellin, E. L., Tamura, K., Vetter, H., Tamura, T., Meisner, J. S., & Frater, R. W. (1988). Passive properties of canine left ventricle: Diastolic stiffness and restoring forces. *Circulation Research*, **62**(6), 1210–1222.
- Notomi, Y., Martin-Miklovic, M. G., Oryszak, S. J., Shiota, T., Deserranno, D., Popovic, Z. B., Garcia, M. J., Greenberg, N. L., & Thomas, J. D. (2006). Enhanced ventricular untwisting during exercise: A mechanistic manifestation of elastic recoil described by Doppler tissue imaging. *Circulation*, **113**(21), 2524–2533.
- Ogoh, S., Sato, K., Okazaki, K., Miyamoto, T., Hirasawa, A., Morimoto, K., & Shibasaki, M. (2013). Blood flow distribution during heat stress: Cerebral and systemic blood flow. *Journal of Cerebral Blood Flow and Metabolism*, **33**(12), 1915–1920.

- Oxborough, D., Shave, R., Warburton, D., Williams, K., Oxborough, A., Charlesworth, S., Foulds, H., Hoffman, M. D., Birch, K., & George, K. (2011). Dilatation and dysfunction of the right ventricle immediately after ultraendurance exercise: Exploratory insights from conventional two-dimensional and speckle tracking echocardiography. *Circulation: Cardiovascular Imaging*, **4**(3), 253–263.
- Parker, J. O., Khaja, F., & Case, R. B. (1971). Analysis of left ventricular function by atrial pacing. *Circulation*, **43**(2), 241–252.
- Parker, K. H., & Jones, C. J. H. (1990). Forward and backward running waves in the arteries: Analysis using the method of characteristics. *Journal of Biomechanical Engineering*, **112**(3), 322–326.
- Patterson, S. W., & Starling, E. H. (1914). On the mechanical factors which determine the output of the ventricles. *The Journal of Physiology*, **48**(5), 357–379.
- Pearson, J., Low, D. A., Stöhr, E., Kalsi, K., Ali, L., Barker, H., & González-Alonso, J. (2011). Hemodynamic responses to heat stress in the resting and exercising human leg: Insight into the effect of temperature on skeletal muscle blood flow. *American Journal of Physiology-Regulatory, Integrative and Comparative Physiology*, **300**(3), R663–R673.
- Pinho, D., Rodrigues, R. O., Faustino, V., Yaginuma, T., Exposto, J., & Lima, R. (2016). Red blood cells radial dispersion in blood flowing through microchannels: The role of temperature. *Journal of Biomechanics*, **49**(11), 2293–2298.
- Plagenhoef, S., Evans, F. G., & Abdelnour, T. (1983). Anatomical data for analyzing human motion. *Research Quarterly for Exercise and Sport*, **54**(2), 169–178.
- Ramanathan, N. L. (1964). A new weighting system for mean surface temperature of the human body. *Journal of Applied Physiology*, **19**(3), 531–533.
- Ross, J., Linhart, J. W., & Braunwald, E. (1965). Effects of changing heart rate in man by electrical stimulation of the right atrium. Studies at rest, during exercise, and with isoproterenol. *Circulation*, **32**(4), 549–558.
- Rovner, A., Smith, R., Greenberg, N. L., Tuzcu, E. M., Smedira, N., Lever, H. M., Thomas, J. D., & Garcia, M. J. (2003). Improvement in diastolic intraventricular pressure gradients in patients with HOCM after ethanol septal reduction. *American Journal of Physiology-Heart and Circulatory Physiology*, **285**(6), H2492–H2499.
- Rowell, L. B. (1993). *Human cardiovascular control*. Oxford Univ. Press.
- Rowell, L. B., Brengelmann, G. L., Blackmon, J. R., & Murray, J. A. (1970). Redistribution of blood flow during sustained high skin temperature in resting man. *Journal of Applied Physiology*, **28**(4), 415–420.
- Rowell, L. B., Brengelmann, G. L., & Murray, J. A. (1969). Cardiovascular responses to sustained high skin temperature in resting man. *Journal of Applied Physiology*, **27**(5), 673–680.
- Rowell, L. B., Detry, J. R., Profant, G. R., & Wyss, C. (1971). Splanchnic vasoconstriction in hyperthermic man—role of falling blood pressure. *Journal of Applied Physiology*, **31**(6), 864–869.
- Sagawa, K., Suga, H., Shoukas, A. A., & Bakalar, K. M. (1977). End-systolic pressure/volume ratio: A new index of ventricular contractility. *American Journal of Cardiology*, **40**(5), 748–753.
- Sawka, M. N., Young, A. J., Pandolf, K. B., Dennis, R. C., & Valeri, C. R. (1992). Erythrocyte, plasma, and blood volume of healthy young men. *Medicine and Science in Sports and Exercise*, **24**(4), 447–453.
- Secomb, T. W. (2016). Hemodynamics. *Comprehensive Physiology*, **6**, 975–1003.
- Shin, S., Ku, Y., Park, M. S., & Suh, J. S. (2004). Measurement of blood viscosity using a pressure-scanning capillary viscosimeter. *Clinical Hemorheology and Microcirculation*, **30**, 467–470.
- Shinsato, T., Miyata, M., Kubozono, T., Ikeda, Y., Fujita, S., Kuwahata, S., Akasaki, Y., Hamasaki, S., Fujiwara, H., & Tei, C. (2010). Waon therapy mobilizes CD34+ cells and improves peripheral arterial disease. *Journal of Cardiology*, **56**(3), 361–366.
- Snyder, G. K. (1971). Influence of temperature and hematocrit on blood viscosity. *American Journal of Physiology*, **220**(6), 1667–1672.
- Starling, M. R. (1993). Left ventricular-arterial coupling relations in the normal human heart. *American Heart Journal*, **125**(6), 1659–1666.
- Stein, E., Damato, A. N., Kosowsky, B. D., Lau, S. H., & Lister, J. W. (1966). The relation of heart rate to cardiovascular dynamics. Pacing by atrial electrodes. *Circulation*, **33**(6), 925–932.
- Stöhr, E. J., González-Alonso, J., Pearson, J., Low, D. A., Ali, L., Barker, H., & Shave, R. (2011). Effects of graded heat stress on global left ventricular function and twist mechanics at rest and during exercise in healthy humans. *Experimental Physiology*, **96**(2), 114–124.
- Stöhr, E. J., González-Alonso, J., & Shave, R. (2011). Left ventricular mechanical limitations to stroke volume in healthy humans during incremental exercise. *American Journal of Physiology-Heart and Circulatory Physiology*, **301**(2), H478–H487.
- Stöhr, E. J., Shave, R. E., Baggish, A. L., & Weiner, R. B. (2016). Left ventricular twist mechanics in the context of normal physiology and cardiovascular disease: A review of studies using speckle tracking echocardiography. *American Journal of Physiology-Heart and Circulatory Physiology*, **311**(3), H633–H644.
- Sunagawa, K., Maughan, W. L., Burkhoff, D., & Sagawa, K. (1983). Left ventricular interaction with arterial load studied in isolated canine ventricle. *American Journal of Physiology-Heart and Circulatory Physiology*, **245**(5), H773–H780.
- Toner, M. M., Drolet, L. L., & Pandolf, K. B. (1986). Perceptual and physiological responses during exercise in cool and cold water. *Perceptual and Motor Skills*, **62**(1), 211–220.
- Trangmar, S. J., Chiesa, S. T., Stock, C. G., Kalsi, K. K., Secher, N. H., & González-Alonso, J. (2014). Dehydration affects cerebral blood flow but not its metabolic rate for oxygen during maximal exercise in trained humans. *The Journal of Physiology*, **592**(14), 3143–3160.

- Trangmar, S. J., & González-Alonso, J. (2017). New insights into the impact of dehydration on blood flow and metabolism during exercise. *Exercise and Sport Sciences Reviews*, **45**(3), 146–153.
- Trudnowski, R. J., & Rico, R. C. (1974). Specific gravity of blood and plasma at 4 and 37 degrees C. *Clinical Chemistry*, **20**(5), 615–616.
- Tsuji, B., Hoshi, Y., Honda, Y., Fujii, N., Sasaki, Y., Cheung, S. S., Kondo, N., & Nishiyasu, T. (2019). Respiratory mechanics and cerebral blood flow during heat-induced hyperventilation and its voluntary suppression in passively heated humans. *Physiological Reports*, **7**(1), e13967.
- Van Mil, A. C. C. M., Pearson, J., Drane, A. L., Cockcroft, J. R., McDonnell, B. J., & Stöhr, E. J. (2016). Interaction between left ventricular twist mechanics and arterial haemodynamics during localised, non-metabolic hyperaemia with and without blood flow restriction. *Experimental Physiology*, **101**(4), 509–520.
- Watanabe, K., Stöhr, E. J., Akiyama, K., Watanabe, S., & González-Alonso, J. (2020). Dehydration reduces stroke volume and cardiac output during exercise because of impaired cardiac filling and venous return, not left ventricular function. *Physiological Reports*, **8**(11), e14433.
- Wexler, L., Bergel, D. H., Gabe, I. T., Makin, G. S., & Mills, C. J. (1968). Velocity of blood flow in normal human venae cavae. *Circulation Research*, **23**(3), 349–359.
- White, M. D. (2006). Components and mechanisms of thermal hyperpnea. *Journal of Applied Physiology*, **101**(2), 655–663.
- Wiggers, C. J. (1923). *Modern aspects of the circulation in health and disease*. Lea & Febiger.
- Wilson, T. E., Tollund, C., Yoshiga, C. C., Dawson, E. A., Nissen, P., Secher, N. H., & Crandall, C. G. (2007). Effects of heat and cold stress on central vascular pressure relationships during orthostasis in humans. *The Journal of Physiology*, **585**(1), 279–285.
- Yotti, R., Bermejo, J., Antoranz, J. C., Desco, M. M., Cortina, C., Rojo-Álvarez, J. L., Allué, C., Martín, L., Moreno, M., Serrano, J. A., Muñoz, R., & García-Fernández, M. A. (2005). A noninvasive method for assessing impaired diastolic suction in patients with dilated cardiomyopathy. *Circulation*, **112**(19), 2921–2929.

Additional information

Data availability statement

The data that support the findings of this study are available from the corresponding author upon reasonable request.

Competing interests

No conflicts of interest, financial or otherwise, are declared by the author(s).

Author contributions

K.W. and J.G.-A. conceived and designed the study. K.W., N.K.E., O.G., K.A., S.W. and J.G.-A. were involved in data collection. K.W., N.K.E., K.A., S.W. and J.G.-A. were involved in data analysis and interpretation. All authors revised manuscript for important intellectual content. All authors approved the final version of the manuscript and agree to be accountable for all aspects of the work in ensuring that questions related to the accuracy or integrity of any part of the work are appropriately investigated and resolved. All persons designated as authors qualify for authorship, and all those who qualify for authorship are listed.

Funding

This study was conducted at the Centre for Human Performance, Exercise and Rehabilitation, Brunel University London, between March 2017 and March 2018 and was partially supported by grants from the Ministry of Education, Culture, Sports, Science and Technology of Japan (JSPS KAKENHI) grant numbers 19K20034 and 21K17582.

Acknowledgments

We sincerely thank all the participants for their commitment throughout the study. In addition, we would like to thank Tom Howes and Morvarid Osmani for their technical support and assistance and to Prof. Eric J. Stöhr for his help with the cardiac mechanics analysis.

Keywords

cardiac output, passive hyperthermia, peripheral blood flow

Supporting information

Additional supporting information can be found online in the Supporting Information section at the end of the HTML view of the article. Supporting information files available:

Peer Review History